Numerical methods for the simulation of salt migration in regional groundwater flow

E.S. van Baaren

Interim Master's Thesis

December 2006

Thesis Committee:
Dr. ir. F.J. Vermolen (Delft University of Technology)
Dr. ir. C. Vuik (Delft University of Technology)
Prof. dr. ir. P. Wesseling (Delft University of Technology)
Dr. ir. W.J. Zaadnoordijk (Royal Haskoning)

Abstract

Dit is de samenvatting

Contents

Chapter 1

Introduction

In the Netherlands, the effects of the changing climate become more and more visible. Rain falls in higher concentrations, the sea level rises and the discharge of rivers increases. The question rises what the effects of these phenomena will exactly look like in the future. And more precisely will the salt concentration in the groundwater change due to these effects. It is important to be able to answer this question on a very local scale. For the farmer it is important to know whether the ditch becomes to salt to be drinking water for his cattle and for the waterworks it is interesting to know if they can still use a certain source for tap water in ten years.

In coastal areas, density variation has significant influence on groundwater flow. The model that has to be developed will describe variable density groundwater flow through a saturated porous medium. It is of a coupled problem of groundwater flow and concentration of a solute. The first differential equation describes the freshwater head as function of location and time, the second describes the solute transport. These equations are coupled processes and have to be solved jointly.

First the model description will be given with the basic assumptions and differential equations for the groundwater flow and and solute transport.

Introduction is nog niet af. [1][2]

Chapter 2

Model description

2.1 Basic Assumptions

Some assumptions are made in order to simplify the simulation of the groundwater flow and the distribution of the concentration. In the subsurface aquifers are separated by aquitards.

An aquifer is a body of rock or sediment that is sufficiently porous and permeable to store, transmit and yield significant quantities of groundwater to wells and springs. It is assumed that aquifers have a relatively small slope. In most aquifers there are no pumping wells, there is no strongly varying aquifer thickness and no strong water recharge. If they are present, these vertical disturbancies will usually become negligible over a horizontal distance of the order of magnitude of the aquifer thickness. In these cases it is assumed that the vertical resistane in an aquifer can be neglected. This assumption is known as the Dupuit-Forchheimer assumption. Use of this assumption turns a three-dimensional groundwater flow problem into a two-dimensional problem.

An aquitard is a geologic formation that is not permeable enough to yield significant amounts of water to wells, but on a regional scale can supply significant water to the underlying or overlaying aquifers. In an aquitard only vertical velocity is assumed, the horizontal velocity of the flow is zero. As displayed in Figure 2.1, the number of aquitards is assumed to be equal to the number of aquifers minus one. Below the last aquifer there is a aquiclude, which is an impermeable body of rock that may absorb water slowly but does not transmit it. The first aquifer is only assumed for the model to be the last subsurface layer.

The porous subsurface is fully saturated with water, no other fluids or gasses that cannot mix with water are present. The flow is assumed to be laminar and isothermal conditions prevail. The groundwater is incompressible hence solenoidal. In the differential equation for solute transport the diffusive approach to dispersive transport based on Fick's law can be applied.
[3] [4] [5]

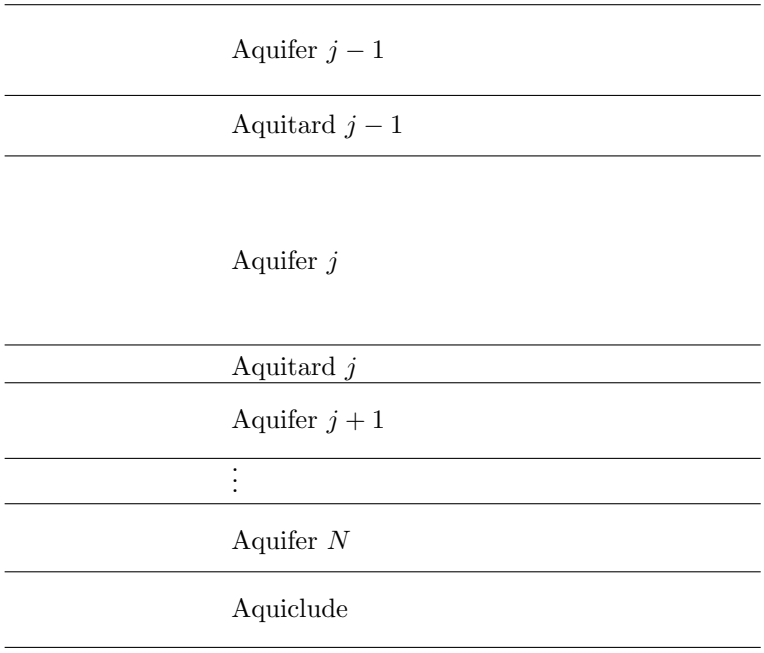

Figure 2.1: Aquifers and aquitards: the layers of the subsurface.

2.2 Flow equation in terms of freshwater head

The variable-density groundwater flow equation is expressed in terms of the equivalent freshwater head and fluid density instead of fluid pressure and fluid density. The freshwater head is defined as

$$h_f = \frac{p}{\rho_f g} + z$$

with p the pressure of the groundwater, ρ_f the density of freshwater, g the acceleration due to gravity and z the vertical coordinate of the location of measure. It can also be explained as the elevation above an arbitrary datum of the water surface in a piezometer tube filled over its full height with freshwater. In Figure 2.2 the difference between the freshwater head and hydraulic head is explained. Fluids flow down a hydraulic gradient, from points of higher to lower hydraulic head. The quantity of head is expressed in terms of a length of water.

Formulation of the flow equation in terms of freshwater head causes no increase in complexity and allows the use of existing software with relatively little modification.

2.2.1 Continuity of mass flow

Define a control volume as in Figure 2.3 in order to derive the conservation of mass flow.

The mass flow $\dot{m}$ is defined as the amount of mass flowing through the control volume per unit time. For directions x, y and z the mass flow is respectively $\dot{m}_x$, $\dot{m}_y$ and $\dot{m}_z$ and hence the total change of mass flow in the control volume is

$$\dot{m}_{out} - \dot{m}_{in} = \dot{m}_{x_{out}} + \dot{m}_{y_{out}} + \dot{m}_{z_{out}} - \dot{m}_{x_{in}} - \dot{m}_{y_{in}} - \dot{m}_{z_{in}},$$

Continuity of the mass flow for one of the directions the can be defined by the outgoing minus incoming flux q_i in the ith direction multiplied by the density ρ of the water and the surface of the control volume in the ith direction. Consider the mass flow in the x-direction, the continuity equation is

$$\dot{m}_{x_{out}} - \dot{m}_{x_{in}} = \left(\rho_{out} q_{x_{out}} - \rho_{in} q_{x_{in}}\right) \Delta y \Delta z,$$

or

$$\Delta \dot{m}_x = \frac{\Delta(\rho q_x)}{\Delta x} \Delta x \Delta y \Delta z.$$

The mass flow in the y-direction and z-direction are derived equivalent. The total change of mass flow through the control volume can now be written as:

$$\Delta \dot{m} = \left(\frac{\Delta(\rho q_x)}{\Delta x} + \frac{\Delta(\rho q_y)}{\Delta y} + \frac{\Delta(\rho q_z)}{\Delta z} \right) \Delta x \Delta y \Delta z. \tag{2.1}$$

The specific storage S_s is the change in storage and is defined as the amount of water which a given volume of aquifer will produce, provided a unit change in hydraulic head is applied to it. It has units of inverse length. Flow in

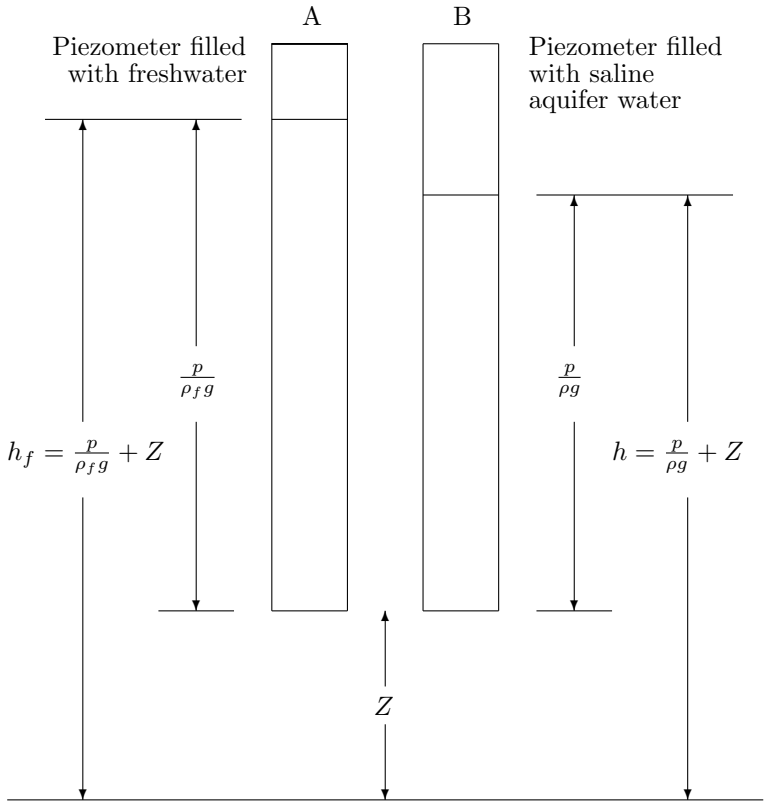

Figure 2.2: Two piezometers, one filled with freshwater and the other with saline water, open to the same point in the aquifer. With h_f the freshwater head, h the hydraulic head, ρ_f the freshwater density, ρ the density of the saline aquifer water and Z the elevation.

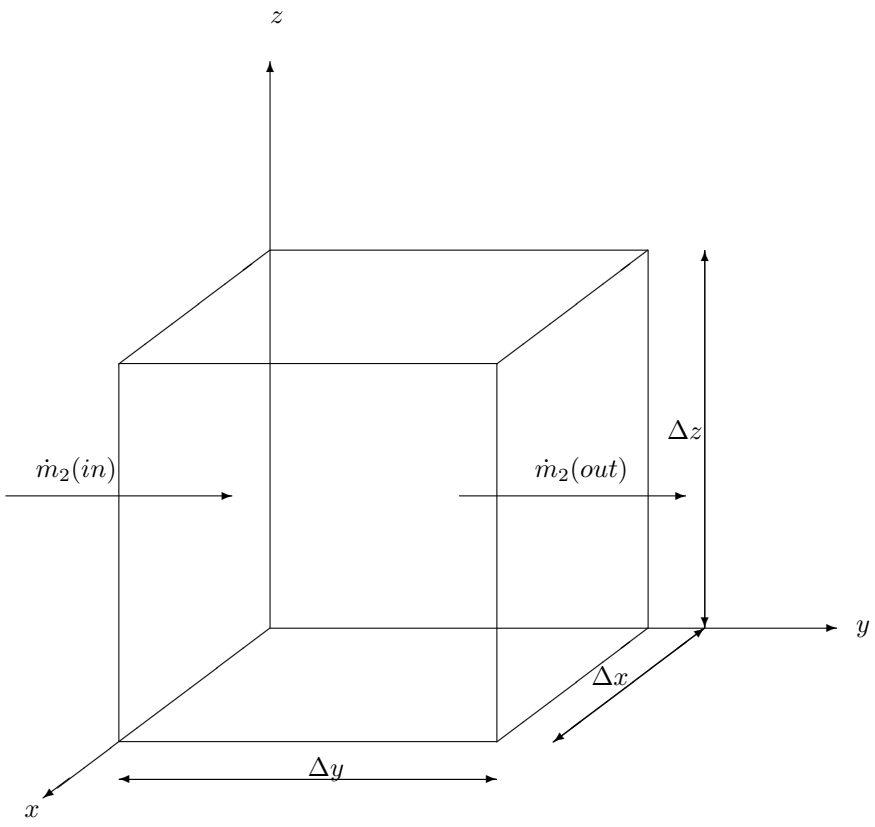

Figure 2.3: Control volume for the mass flow in y-direction.

a porous medium is considered, hence the volume of a control volume of an aquifer ($\Delta x\Delta y\Delta z$) is not necessary the same as the volume of water (V_w) in the same control volume. There is porosity to relate the aquifer volume to the water volume. The specific storage is by definition expressed in terms of V_w, h, x, y and z:

$$S_s = -\frac{\Delta V_w}{\Delta h \Delta x \Delta y \Delta z}.$$

The total change in mass flow can be defined by

$$\Delta \dot{m} = \frac{\Delta V_w \Delta \rho}{\Delta t}.$$

A combination of the previous two equation gives:

$$\Delta \dot{m} = -S_s \frac{\Delta (\rho h)}{\Delta t} \Delta x \Delta y \Delta z. \tag{2.2}$$

Taking both expressions for the change in mass flow (equations (2.1) and (2.2)) together and dividing by $\Delta x\Delta y\Delta z$ results into the continuity equation for the mass flow in a control volume:

$$\left(\frac{\Delta(\rho q_x)}{\Delta x} + \frac{\Delta(\rho q_y)}{\Delta y} + \frac{\Delta(\rho q_z)}{\Delta z} \right) = -S_s \frac{\Delta (\rho h)}{\Delta t}. \tag{2.3}$$

When a source or sink is present Equation (2.3) becomes:

$$\frac{\Delta(\rho q_x)}{\Delta x} + \frac{\Delta(\rho q_y)}{\Delta y} + \frac{\Delta(\rho q_z)}{\Delta z} + \rho q' = -S_s \frac{\Delta (\rho h)}{\Delta t}, \tag{2.4}$$

with q' the volumetric flow rate per unit volume of aquifer representing sources and sinks. It has units of invers time. Taking limits results in:

$$\lim_{\Delta t \to 0, \Delta x \to 0, \Delta y \to 0, \Delta z \to 0} \left(\frac{\Delta(\rho q_x)}{\Delta x} + \frac{\Delta(\rho q_y)}{\Delta y} + \frac{\Delta(\rho q_z)}{\Delta z} + \rho q' \right) = \frac{\partial(\rho q_x)}{\partial x} + \frac{\partial(\rho q_y)}{\partial y} + \frac{\partial(\rho q_z)}{\partial z} + \rho q',$$

$$\lim_{\Delta t \to 0, \Delta x \to 0, \Delta y \to 0, \Delta z \to 0} \left(-S_s \frac{\Delta (\rho h)}{\Delta t} \right) = -S_s \frac{\partial (\rho h)}{\partial t}.$$

And the differential equation for the continuity of mass flow becomes:

$$\frac{\partial(\rho q_x)}{\partial x} + \frac{\partial(\rho q_y)}{\partial y} + \frac{\partial(\rho q_z)}{\partial z} + \rho q' = -S_s \frac{\partial (\rho h)}{\partial t}. \tag{2.5}$$

In order to rewrite Equation (2.5) in terms of freshwater head, define the freshwater head

$$h_f = \frac{p}{\rho_f g} + z,$$

and the (hydraulic)water head

$$h = \frac{p}{\rho g} + z,$$

and eliminate the pressure in the above equations to obtain the relation

$$h = \frac{\rho_f}{\rho} h_f + \frac{\rho - \rho_f}{\rho} z.$$

The right-hand side of Equation (2.5) can now be written as:

$$-S_s \frac{\partial (\rho h)}{\partial t} = -S_s \left(\rho_f \frac{\partial h_f}{\partial t} + z \frac{\partial \rho}{\partial t} \right).$$

Note that the density is written as a function of the concentration (C) of a solute (for example salt) because the equation for Solute Transport in Chapter 2.3 is expressed in terms of concentration. The relation between those two parameters is also explained in Chapter 2.3. Under isothermal conditions and use of the Chain Rule for differentiating on $\rho = \rho(C)$, the groundwater flow equation expressed in terms of the freshwater head is:

$$-\frac{\partial (\rho q_x)}{\partial x} - \frac{\partial (\rho q_y)}{\partial y} - \frac{\partial (\rho q_z)}{\partial z} + \rho q' = S_s \left(\rho_f \frac{\partial h_f}{\partial t} + z \frac{\partial \rho}{\partial C} \frac{\partial C}{\partial t} \right). \tag{2.6}$$

The left-hand side of Equation (2.6) is the net flux of mass through the faces of the control volume plus the rate at which mass enters from sources or leaves through sinks located in the control volume. The right-hand side is the time rate of change in the mass stored in the control volume over a given period. The recharge term q' has dimension $[1/s]$ and is the sum of four distinctive components, depending on the origin of the water:

$$q' = q_a + q_l + q_r + q_s,$$

with

q_l	recharge due to leakage
q_r	recharge from rivers canals and drains
q_s	recharge from sources or sinks
q_a	recharge from the top-system (precipitations, shallow drainage system etc.)

q_l is determined by interpolation between the diffent aquifers and the resistance of the aquitards. q_r, q_s and q_a are, possibly nonlinear, functions of the unknown waterhead and some other known parameters.

[4][6]

2.2.2 Darcy's law

Darcy's law describes the flow of a fluid through a porous medium. For variable density it is given by:

$$\begin{pmatrix} q_x \\ q_y \\ q_z \end{pmatrix} = -\frac{1}{\mu} \begin{pmatrix} \kappa_{xx} & \kappa_{xy} & \kappa_{xz} \\ \kappa_{yx} & \kappa_{yy} & \kappa_{yz} \\ \kappa_{zx} & \kappa_{zy} & \kappa_{zz} \end{pmatrix} \begin{pmatrix} \frac{\partial p}{\partial x} \\ \frac{\partial p}{\partial y} \\ \frac{\partial p}{\partial z} + \rho g \end{pmatrix}, \tag{2.7}$$

with κ, the intrinsic permeability. By definition the pressure in terms of the freshwater head is given by:

$$p = \rho_f g (h_f - z), \tag{2.8}$$

with z upward positive.

For the same reasons as for the continuity of mass flow, Darcy's law is rewritten in terms of freshwaterhead and freshwater hydraulic conductivity. Define the freshwater hydraulic conductivity as

$$k_{f_{ij}} = \frac{\kappa_{ij} \rho_f g}{\mu_f}.$$

The derivatives of the pressure can be calculated as

$$\frac{\partial p}{\partial x} = \rho_f g \frac{\partial h_f}{\partial x},$$

$$\frac{\partial p}{\partial y} = \rho_f g \frac{\partial h_f}{\partial y},$$

$$\frac{\partial p}{\partial z} = \rho_f g \left(\frac{\partial h_f}{\partial z} - 1 \right),$$

hence Equation (2.7) becomes

$$\begin{pmatrix} q_x \\ q_y \\ q_z \end{pmatrix} = - \begin{pmatrix} k_{f_{xx}} & k_{f_{xy}} & k_{f_{xz}} \\ k_{f_{yx}} & k_{f_{yy}} & k_{f_{yz}} \\ k_{f_{zx}} & k_{f_{zy}} & k_{f_{zz}} \end{pmatrix} \begin{pmatrix} \frac{\partial h_f}{\partial x} \\ \frac{\partial h_f}{\partial y} \\ \frac{\partial h_f}{\partial z} + \frac{\rho - \rho_f}{\rho_f} \end{pmatrix}. \tag{2.9}$$

This is Darcy's law for variable density expressed in freshwater head.
[3][7]

2.2.3 Groundwater flow equation

Substitution of Darcy's law (Equation (2.9)) in the equation for conservation of mass (Equation (2.6)) results in the general groundwater flow equation in terms of fresh groundwater head and density:

$$\begin{aligned} &\frac{\partial}{\partial x}\left(\rho\left(k_{f_{xx}}\frac{\partial h_f}{\partial x} + k_{f_{xy}}\frac{\partial h_f}{\partial y} + k_{f_{xz}}\left(\frac{\partial h_f}{\partial z} + \frac{\rho - \rho_f}{\rho_f}\right)\right)\right) + \\ &\quad + \frac{\partial}{\partial y}\left(\rho\left(k_{f_{yx}}\frac{\partial h_f}{\partial x} + k_{f_{yy}}\frac{\partial h_f}{\partial y} + k_{f_{yz}}\left(\frac{\partial h_f}{\partial z} + \frac{\rho - \rho_f}{\rho_f}\right)\right)\right) + \\ &\quad + \frac{\partial}{\partial z}\left(\rho\left(k_{f_{zx}}\frac{\partial h_f}{\partial x} + k_{f_{zy}}\frac{\partial h_f}{\partial y} + k_{f_{zz}}\left(\frac{\partial h_f}{\partial z} + \frac{\rho - \rho_f}{\rho_f}\right)\right)\right) + \rho q' = \\ &\quad = S_s\left(\rho_f \frac{\partial h_f}{\partial t} + z\frac{\partial \rho}{\partial C}\frac{\partial C}{\partial t}\right). \end{aligned} \tag{2.10}$$

The boundary and initial conditions for the groundwater head can be found in the Chapter Boundary and Initial conditions (chapter 2.5).

Parameters of the flow equation
According to [5], the ranges of values of the specific storage S_s are independent of time but do dependent on location. For different materials they are:

Material	Specific storage S_s (m^{-1})
Loose sand	$1.0 * 10^{-3} - 4.9 * 10^{-4}$
Dense sand	$2.0 * 10^{-4} - 1.3 * 10^{-4}$
Dense sandy gravel	$1.0 * 10^{-4} - 4.9 * 10^{-5}$
Rock, fissured, jointed	$6.9 * 10^{-5} - 3.3 * 10^{-6}$

Table : Ranges of values of S_s, adapted from Domenico 1972. [5]

Further, ρ_f is constant under isothermal conditions:

Temperature (℃)	Freshwater density ρ_f $(kg/liter)$
4	1.000
20	0.9982
40	0.9922
80	0.9718

Table : Ranges of values of ρ_f

The values of the freshwater hydraulic conductivity tensor k_f are all known and assumed to be continuous and differentiable. The control volume $\Delta x \Delta y \Delta z$ is aligned with coordinate directions that are neither parallel nor normal to the aquifer. Often the aquifers are horizontal and in that case the non-diagonal elements are zero. But in order to be able to use this model in all cases, for example in the case of a lateral moraine where the groundlayers are not in the same direction as the water flow, the complete tensor is used.

The model for solute transport will deliver the values for the concentration C, and hence the density ρ, each time step for each location. in [8] the following formula is experimentally derived:

$$\rho = 1 + 5.05 * 10^{-7} * RE - 6.5 * 10^{-6} \left(T - 4 + 2.2 * 10^{-4} RE\right) \tag{2.11}$$

T is the temperature in ℃. RE is the residue on evaporation at 180℃in mg/kg which can be calculated from chlorinity ($mg\ Cl^-$ water):

$$RE = 1.805 Cl^- + 30$$

Note that ρ is the density in water in kg/l.

The freshwater head h_f is the output variable which is determined by this differential equation.

2.3 Solute transport

In general situations, the direction of flow is variable. Take again the control volume as defined in Figure 2.3 but now consider the change of mass in time ($\dot{m}$) expressed in the Darcy velocity $\mathbf{q}$ and the concentration C of a solute (salt) in the water. The control volume $\Delta x \Delta y \Delta z$ is aligned with coordinate directions that are neither parallel nor normal to the aquifer. Thus the Darcy velocity has

components in all three dimensions. We will allow for the possible presence of sources or sinks within the control volume.

First the change of mass in time due to advection and sources or sinks is developed. For simplicity, assume that storage effects involve only changes in fluid density within a rigid porous framework. The net inflow minus outflow of solute mass in the x-direction for the control volume is:

$$\dot{m}_x = -\frac{\Delta(q_x C)}{\Delta x}\Delta x\Delta y\Delta z,$$

The y-direction and z-direction are derived equivalent. And the total change of mass in time due to advection and sources or sinks is:

$$\dot{m} = -\left(\frac{\Delta(q_x C)}{\Delta x} + \frac{\Delta(q_y C)}{\Delta y} + \frac{\Delta(q_z C)}{\Delta z}\right)\Delta x\Delta y\Delta z + Q_{so}C_s, \tag{2.12}$$

C_s represents the concentration of the solute in the water that is added or withdrawn and Q_{so} denotes the volumetric rate at which water is added or removed, where a positive sign indicates a source and a negative sign a sink. The term $Q_{so}C_s$ thus represents the net rate at which solute mass is added to or removed from the control volume by the source or sink, expressed in units of mass per unit time.

Assume further that the solute carried in advective transport remains completely within the moving water. In particular there is no diffusion of solute into and from sections of the pore space that may contain (nearly) static water. Static water is the term used for non-moving water that doesnot contribute to the continuity of mass. Then the volume of water containing solute in the control volume $\Delta x\Delta y\Delta z$ is $\theta\Delta x\Delta y\Delta z$. With θ the dimensionless effective porosity independent on time but dependent on the spatial coordinates. The mass of solute in the control volume at any time is $\theta\Delta x\Delta y\Delta z C$ with C the average concentration in the control volume. Thus the rate at which the mass changes with time can also be written as:

$$\dot{m} = \theta\frac{\Delta C}{\Delta t}\Delta x\Delta y\Delta z. \tag{2.13}$$

Combination of the equations (2.12) and (2.13), dividing both sides by $\Delta x\Delta y\Delta z$ and taking the limits of Δt, Δx, Δy and Δz to 0 results in:

$$-\nabla\cdot(\mathbf{q}C) + q_{so}C_s = \theta\frac{\partial C}{\partial t}|_{\text{due to advection and sources/sinks}}, \tag{2.14}$$

with q_{so} the volumetric flow rate per unit volume of the aquifer due to the fluid source or sink.

Second, the change of mass in time due to dispersion is developed. For the three-dimensional case, the dispersion coefficient tensor contains nine terms. The dispersive transport in terms of mass per unit time in the control volume is derived in [9] and given by:

$$\dot{m}_i = -\left(D_{ix}\frac{\Delta C}{\Delta x} + D_{iy}\frac{\Delta C}{\Delta y} + D_{iz}\frac{\Delta C}{\Delta z}\right)\theta\Delta x_j\Delta x_k.$$

The difference between inflow and outflow of mass due to dispersion can be derived by multiplying above equation by $\frac{\Delta x_i}{\Delta x_i}$, again using $\dot{m} = \dot{m}_1 + \dot{m}_2 + \dot{m}_3$

and taking the limits for Δt, Δx, Δy and Δz to 0. This results in:

$$\nabla \cdot (\theta D \nabla C) = \theta \frac{\partial C}{\partial t}|_{\text{due to dispersion}}, \tag{2.15}$$

Combination of the equations (2.14) and (2.15) results in the transport equation of solute mass in groundwater:

$$\theta \frac{\partial C}{\partial t} = \nabla \cdot (\theta D \nabla C) - \nabla \cdot (\mathbf{q} C) + q_{so} C_s. \tag{2.16}$$

When the assumption of the divergence free groundwater is used, Equation (2.16) becomes

$$\theta \frac{\partial C}{\partial t} = \nabla \cdot (\theta D \nabla C) - \nabla \cdot (\mathbf{q} C) + q_{so} C_s, \tag{2.17}$$

with

$$D\nabla C = \begin{pmatrix} D_{xx} & D_{xy} & D_{xz} \\ D_{yx} & D_{yy} & D_{yz} \\ D_{zx} & D_{zy} & D_{zz} \end{pmatrix} \begin{pmatrix} \frac{\partial C}{\partial x} \\ \frac{\partial C}{\partial y} \\ \frac{\partial C}{\partial z} \end{pmatrix}.$$

Solute mass is transported in porous media by the flow of groundwater (advection), molecular diffusion and mechanical dispersion. The first term of the right-hand side of Equation (2.17) is a combined term of molecular diffusion and dispersion. The order of diffusion is $10^{-9}\ m^2/day$, the order of dispersion is $3 * 10^{-3}\ m^2/day$. The diffusion becomes only important when the velocity field is zero because the order of the dispersion and advection effect are much bigger than the order of the diffusion effect. The second term of the right-hand side is the advection term and is of the order $3 * 10^{-2}\ m/day$. Note that there is no reaction term in the differential equation because only salt in water is considered.

Parameters of the solute transport equation
The Darcy velocity vector $\mathbf{q}$ is determined by the groundwater flow Equation (2.10). The porosity θ is a subsurface property and hence depends on the spatial coordinates. The porosity θ is known for each part of the ground. The dispersion coefficient tensor D is anisotropic but all elements of the tensor are known and the source/sink term $q_{so}C_s$ is known. The concentration C as function of time and location has to be solved with this differential equation.

2.4 The coupled process

The movement of groundwater (Equation (2.10)) and the transport of solutes (equation(2.17)) in the aquifer are coupled processes and the two equations must be solved as a coupled problem. This coupled process is shown in Figure 2.4.

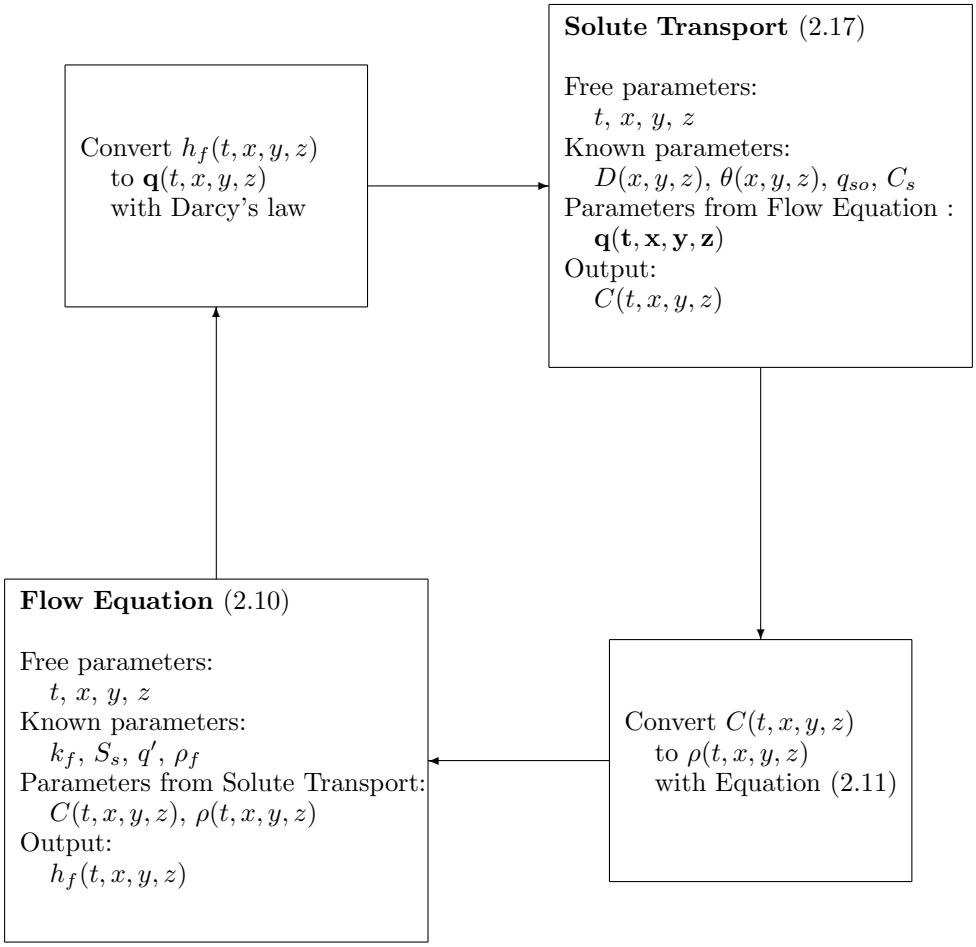

Figure 2.4: The coupled process for the solving of the equations for solute transport (2.17) and groundwater flow (2.10).

2.5 Boundary and Initial conditions

In order to make the solution of the equations (2.10) and (2.17) unique and well-posed, a number of conditions (boundary and initial) should be given. For a unique solution, it is necessary to prescribe exactly one boundary condition at each part of the boundary. We consider the following boundary conditions:

Dirichlet boundary
A Dirichlet boundary Γ_0 is such that the value of the head or the concentration is specified at all points along the boundary Γ_0. For example, for the concentration the Dirichlet boundary conditon is:

$$C(\mathbf{x}) = g_0(\mathbf{x}) \qquad \mathbf{x} \in \Gamma_0. \tag{2.18}$$

A physical example of an Dirichlet boundary might be a fully penetrating stream or other surface-water body on the boundary of the model domain along which head or concentration is specified. Another example might be a drain operating at a specified water level in the interior of the model domain.

Neumann boundary
On the Neumann boundary Γ_1 a condition in which the gradient of the dependent variable normal to the boundary is specified. For example, for the concentration the Neumann boundary condtion for the boundary Γ_1 is:

$$(D \cdot \nabla C) \cdot \mathbf{n} = g_1(\mathbf{x}) \qquad \mathbf{x} \in \Gamma_1. \tag{2.19}$$

For groundwater flow this boundary condition results in a specified flux of water into or out of the modeled area. For solute transport the concentration gradient is specified normal to the boundary. A physical example is an impermeable boundary where the gradients of head and concentration are zero at the boundary. An example of a nonzero Neumann boundary in flow simulation might be a surface-water body from which seepage occurs at a prescribed rate.

Robbins boundary
On the Robbins boundary Γ_3 a mixed condition is specified:

$$(D \cdot \nabla C) \cdot \mathbf{n} + \sigma C = g_2(\mathbf{x}) \qquad \mathbf{x} \in \Gamma_2. \tag{2.20}$$

Here a flow might be prescribed in which both the dispersive and advective contributions are taken into account. Another example of this mixed boundary condition which gives a relation between a flux and a unknown, is the boundary condition due to the linearization of a radiation condition.

Note that the advection term in Equation (2.17) might strongly dominate the dispersive term. For a pure advection equation, boundary conditions should only be given at inflow and not at outflow boundaries. Since for the advection-dispersion equation boundary conditions must be given at the outflow, those boundary conditions are recommended that influence the solution as little as possible. In general this means that at the outflow boundary one usually applies natural boundary conditions. Dirichlet boundary conditions may result in unwanted wiggles.

For the instationary problem, initial conditions for both flow (freshwater head) and transport (concentration and velocity) must be specified.

[3] [6] [9]

Chapter 3

Numerical solution methods

Equations (2.10) and (2.17) are both solved numerically. The Groundwater Flow equation is solved by the Finite Element Method and the equation for Solute Transport is solved by both the Finite Element Method, the Finite Difference Method and the Finite Volume Method. The problem for solute transport is a three dimensional problem. The used groundwater flow equation is described in Chapter 4.

For salt concentrations in an aquifer non-smooth initial conditions or sources are unlikely. However to be able to use this model also for thermal problems it might be necessary to investigate higher order problems.

In the Sections 3.2, 3.3 and 3.4 the numerical methods FE, FV and FD are discussed. These methods belong to one of the three types of numerical methods. In Section 3.10 the IFALT method is discussed, which is an analytical method but uses numerical methods to solve the dispersion term and the inverse Laplace Transform. All types have their own characteristics. The first type is the class of Eulerian methods, these methods attemp to solve the advection dispersion equation on a fixed grid. Well-known examples are the methods presented in the Sections 3.2, 3.3 and 3.4. The second type are the Lagrangian methods, that employ a moving coordinate system to obtain solutions, mainly using particle tracking as implementation method as mentioned in Section 3.9. The third type are the mixed Eulerian-Lagrangian methods. A common example is the Method of Characteristics. IFA (Section 3.10) belongs to the Eulerian methods. ?(klopt dat wel, wat hij gebruikt de method of characteristics en dat is een gecombineerde methode?)?

3.1 Grid

The differential equations (2.10) and (2.17) need to be discretized on a suitable grid. Within a grid the choice for the arrangements of unknowns has to be made. The most common types of grids are:

- Cartesian grids,
- Boundary-fitted, logically rectangular grids,
- Block-structured boundary-fitted grids,

- Unstructured grids,
- Self-adaptive grids.

For simple domains Ω and simple boundaries Γ, Cartesian grids are numerically convenient, see Figure ... for a two-dimensional example. A two-dimensional boundary-fitted, logically rectangular grid can be found in ... . The use of boundary fitted coordinates makes the boundary of the domain a coordinate line. This usually leads to a reformulation of the problem in general curvilinear coordinates. This solves one problem, bus introduces another because usually the partial differential equation becomes complex very soon. Block-structured boundary-fitted grids are used if the given domain cannot reasonably be mapped to a rectangular domain, but can be decomposed into a finite number of subdomains each of which can be covered with a boundary-fitted grid. See Figure... . Unstructured grids have the advantage that automatic mesh generation is much easier than the block-structured grids for complicated domains. Finally, self-adaptive grids are constructed automatically during the solution process according to an error estimator that takes the behavior of the solution into account.

In principle, any type of grid can be used with any type of discretization approach. For each of the numerical methods finite elements, finite differences and finite volumes, the most suitable type of grid is used. Aquifers are often simple shaped domains but a local grid refinement is requested near for example watercourses, sources or drains. Hence for the numerical methods in the Chapters 3.2, 3.4 and 3.3 the optimal grid is the block-structured grid (not boundary fitted).

A common way to define the arrangements of unknowns is at the vertices of a grid (vertex-centered location of unknowns) or at the cell centers (cell-centered location of unknowns). A staggered grid is an ordinary example of choosing different locations for different types of unknowns or components. Often a staggered grid leads to smaller errors in the numerical approximation. All three arrangements of unknowns can be found in Figure 3.1. According to [10], it is hard to say which location of unknowns and which location of the discretization is best in general. Often choices depend on the type of boundary conditions. It should be able to use all kinds of boundary conditions for both the groundwater flow equation and the equation for solute transport so for each method the most general grid is chosen.

[10]

3.2 Finite Elements

3.2.1 Grid

For the Finite Element Method a vertex-centered grid is chosen. The common element shape for this method in three dimensions is the linear shaped tetrahedron, see Figure 3.2. On the other hand a bilinear prisma shaped element as in Figure 3.3 may be more suitable for the used numerical model for the flow equation. This prisma shaped element may be seen as three coupled tetrahedrons as can be seen in Figure E.1.

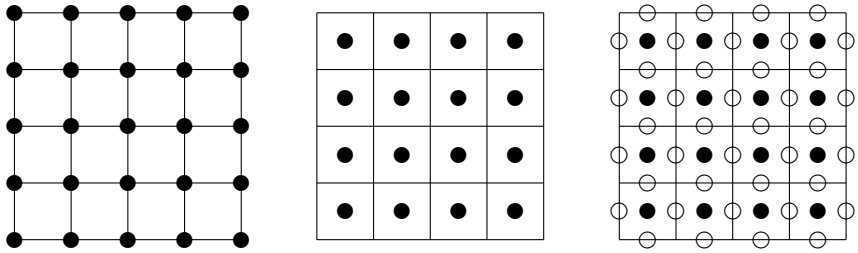

Figure 3.1: Three arrangements of unknowns in a two dimensional Cartesian grid: a) a vertex-centered grid, b) a cell-centered grid, c) a staggered grid.

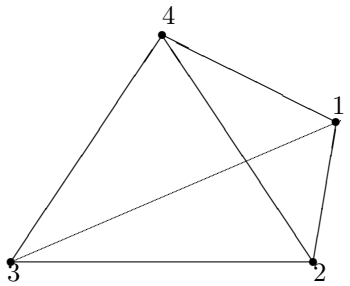

Figure 3.2: Tetrahedron: element of the three dimensional mesh for the Finite Element Method with the four vertices.

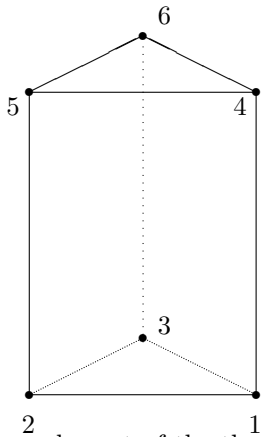

Figure 3.3: Prisma: element of the three dimensional mesh for the Finite Element Method with the six vertices.

3.2.2 Groundwater equation

3.2.3 Solute transport

The Finite Element scheme for the linear three-dimensional tetrahedron shaped element of Figure 3.2 is derived. This scheme can easily be changed for the bilinear isoparametric prisma of Figure 3.3. In that case, the basis function of Equation (3.16) becomes $\phi_i(\mathbf{x}) = a_0^i + a_1^i x + a_2^i y + a_3^i z + a_4^i xy + a_5^i xyz$.

Spatial discretization: Standard Galerkin Approach

Galerkin's method for the spatial discretization results into a system of ordinary differential equations which can be represented by:

$$M\frac{dC_h}{dt} = SC_h + q_h,$$

with M the mass matrix and S the stiffness matrix of the corresponding problem. In order to derive this set of ODE's, split the boundary into three parts and remember Equation (2.17) with boundary and inital conditions:

$$\begin{cases} -\nabla \cdot (\theta D \nabla C) + \mathbf{q} \cdot \nabla C + \theta \frac{\partial C}{\partial t} = q_{so} C_s \\ C|_{\Gamma_1} = g_1(\mathbf{x}) \\ ((\theta D \nabla C) \cdot \mathbf{n})\,|_{\Gamma_2} = g_2(\mathbf{x}) \\ (\sigma C + (\theta D \nabla C \cdot \mathbf{n}))\,|_{\Gamma_3} = g_3(\mathbf{x}) \qquad \sigma \geq 0 \\ C(\mathbf{x}, t_0) = C_0(\mathbf{x}) \end{cases} \tag{3.1}$$

with D the symmetric matrix

$$D = \begin{pmatrix} D_{xx} & D_{xy} & D_{xz} \\ D_{yx} & D_{yy} & D_{yz} \\ D_{zx} & D_{zy} & D_{zz} \end{pmatrix}.$$

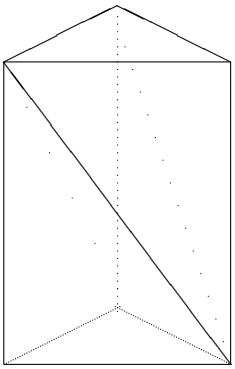

Figure 3.4: The prisma exists of three linear shaped tetrahedrons. Two of them have the same dimensions.

Note that the differential equation is linear, because the coefficients are independent of the solution. The spatial discretization is based on the Finite Element Method. Consider a bounded domain Ω in $\mathbb{R}^3$ and subdivide it into tetrahedrons. Define the approximation C^n of the unknown solution C by a finite linear combination of basis functions:

$$C^n(\mathbf{x},t) = \sum_{j=1}^{n} C_j(t)\phi_j(\mathbf{x}) + \sum_{j=n+1}^{n+n_B} g_1(\mathbf{x})\phi_j(\mathbf{x}), \tag{3.2}$$

with n the number of unknowns, n_B the number of boundary elements and

Definition 1 *The linearly independent basis functions ϕ_j are defined as:*

1. *$\phi_i(\mathbf{x})$ linear per tetrahedron,*
2. *$\phi_i(\mathbf{x^j}) = \delta_{ij}$.*

Under the conditions of Definition 1, $\{\phi_i\}$ are linearly independent, $\{\phi_i\}$ span a complete function space, and hence $lim_{n_B\to\infty} C^n(\mathbf{x},t) = C(\mathbf{x},t)\ \forall \mathbf{x} \in \mathbb{R}^n$.

In order to derive the system of ordinary differential equations, start with multiplying the differential equation in (3.1) by a time-independent test function η. This function η satisfies the homogeneous essential boundary condition $\eta|_{\Gamma_1} = 0$ and has to an element of the Hardy space H_1. In complex analysis, H_1 is is analogues of the L_1 space of functional analysis. The L_1 space is defined as

$$L_1(\Omega) = \{f : \Omega \to \mathbb{R} :\ \text{f is measurable and } \int_\Omega |f| d\mu < \infty \text{ and } f \neq 0 \text{ almost everywhere}\}$$

More information about this space can be found in [11].

Then, integrate over the domain Ω:

$$\int_\Omega \left\{ -\nabla \cdot (\theta D \nabla C) + \mathbf{q} \cdot \nabla C + \theta \frac{\partial C}{\partial t} - q_{so} C_s \right\} \eta d\Omega = 0. \tag{3.3}$$

Apply Green's theorem only to the second derivative. Application to the first order term would not result in lower order derivatives, since the first derivative of the concentration would be replaced by a first derivative of the test function.

Green's theorem:
Let Ω be the bounded domain with piecewise smooth boundary Γ. Let c, $\mathbf{u}$ be sufficiently smooth, and n the outward normal. Then

$$\int_\Omega c \nabla \cdot \mathbf{u} d\Omega = -\int_\Omega (\nabla c) \cdot \mathbf{u} d\Omega + \int_\Gamma c\mathbf{u} \cdot \mathbf{n} d\Gamma. \tag{3.4}$$

With Green's theorem the second order derivative in Equation (3.3) becomes:

$$-\int_\Omega \{\nabla \cdot (\theta D \nabla C)\} \eta d\Omega = \int_\Omega (\nabla \eta) \cdot (\theta D \nabla C) d\Omega - \int_\Gamma \eta \theta D \nabla C \cdot \mathbf{n} d\Gamma.$$

So Equation (3.3) becomes:

$$\int_\Omega \left((\nabla \eta) \cdot (\theta D \nabla C) + \left(\mathbf{q} \cdot \nabla C + \theta \frac{\partial C}{\partial t} - q_{so} C_s \right) \eta \right) d\Omega - \int_\Gamma \eta \theta D \nabla C \cdot \mathbf{n}\, d\Gamma = 0. \tag{3.5}$$

Substituting the boundary conditions on Γ_2 and Γ_3 (see (3.1)) as well as the essential boundary condition for the test function $\eta|_{\Gamma_1} = 0$ leads to:

$$\int_\Omega \left((\nabla\eta) \cdot (\theta D \nabla C) + (\mathbf{q} \cdot \nabla C)\eta + \theta \frac{\partial C}{\partial t}\eta \right) d\Omega + \int_{\Gamma_3} \sigma C \eta d\Gamma = \\ = \int_\Omega q_{so} C_s \eta d\Omega + \int_{\Gamma_2} g_2 \eta d\Gamma + \int_{\Gamma_3} g_3 \eta d\Gamma. \tag{3.6}$$

Equation (3.6) together with the boundary conditions on Γ_1 ($C|_{\Gamma_1} = g_1(\mathbf{x})$ and $\eta|_{\Gamma_1} = 0$) and the initial condition ($C(\mathbf{x}, t_0) = C_0(\mathbf{x})$), forms the *weak formulation* of (3.1). Approximate C by C^n and substitute (3.2) into (3.6) and substitute $\eta = \phi_i(\mathbf{x})$ for i from 1 to n. This yields the following system of ordinary differential equations (*the Galerkin formulation*): .

$$\frac{d}{dt} \sum_{j=1}^{n} C_j \int_\Omega \theta(\mathbf{x}_j)\phi_j\phi_i d\Omega = \\ = -\sum_{j=1}^{n} C_j \left(\int_\Omega \left(\nabla\phi_i \cdot (\theta(\mathbf{x}_j) D(\mathbf{x}_j) \nabla\phi_j) + (\mathbf{q}(\mathbf{x}_j) \cdot \nabla\phi_j)\, \phi_i \right) d\Omega + \right. \\ \left. \int_{\Gamma_3} \sigma(\mathbf{x}_j)\phi_j\phi_i d\Gamma \right) + \int_\Omega (q_{so}C_s)(\mathbf{x}_j)\phi_i d\Omega + \int_{\Gamma_2} g_2(\mathbf{x}_j)\phi_i d\Gamma + \int_{\Gamma_3} g_3(\mathbf{x}_j)\phi_i d\Gamma \\ - \sum_{j=n+1}^{n+n_B} \int_{\Gamma_3} \sigma g_1(\mathbf{x}_j)\phi_j\phi_i d\Gamma - \sum_{j=n+1}^{n+n_B} \int_\Omega (\nabla\phi_i \cdot (\theta(\mathbf{x}_j) D(\mathbf{x_j}) g_1(\mathbf{x}_j) \nabla\phi_j) + \\ + (\mathbf{q}(\mathbf{x}_j) \cdot (g_1(\mathbf{x}_j)\nabla\phi_j))\phi_i)\, d\Omega \\ \text{for } i \in 1, ..., n. \tag{3.7}$$

This system of n linear ordinary differential Equations with n unknowns can be written in the form

$$M \frac{dC}{dt} = SC + f,$$

with M and S $n \times n$-matrices and $\frac{dC}{dt}$, C and f $n \times 1$-vectors. The elements of M, S and f are:

$$m_{ij} = \int_\Omega \theta(\mathbf{x}_j)\phi_j\phi_i d\Omega, \tag{3.8}$$

$$s_{ij} = -\int_\Omega \left(\nabla\phi_i \cdot (\theta(\mathbf{x}_j) D(\mathbf{x}_j) \nabla\phi_j) + (\mathbf{q}(\mathbf{x}_j) \cdot \nabla\phi_j)\phi_i \right) d\Omega - \int_{\Gamma_3} \sigma\phi_j\phi_i d\Gamma, \tag{3.9}$$

$$f_i = \int_\Omega (q_{so}C_s)(\mathbf{x}_j)\phi_i d\Omega + \int_{\Gamma_2} g_2(\mathbf{x}_j)\phi_i d\Gamma + \int_{\Gamma_3} g_3(\mathbf{x}_j)\phi_i d\Gamma \\ - \int_{\Gamma_3} \sigma \sum_{j=n+1}^{n+n_B} g_1(\mathbf{x}_j)\phi_j\phi_i d\Gamma - \int_\Omega \sum_{j=n+1}^{n+n_B} (\nabla\phi_i \cdot (\theta(\mathbf{x}_j) D(\mathbf{x}_j) g_1(\mathbf{x}_j) \nabla\phi_j) \\ + (\mathbf{q}(\mathbf{x}_j) \cdot (g_1(\mathbf{x}_j)\nabla\phi_j))\phi_i)\, d\Omega. \tag{3.10}$$

The above integrals over the domain are splitted into integrals over the elements in order to make the computations less complicated. With n_e the

number of elements, e_k a typical element, n_{be} the number of boundary elements and Ω^{e_k} the area of element e_k the Equations (3.8), (3.9) and (3.28) become:

$$m_{ij} = \sum_{k=1}^{n_e} \int_{\Omega^{e_k}} \theta(\mathbf{x}_j)\phi_j\phi_i d\Omega, \tag{3.11}$$

$$s_{ij} = -\sum_{k=1}^{n_e} \int_{\Omega^{e_k}} (\nabla\phi_i \cdot (\theta(\mathbf{x}_j)D(\mathbf{x}_j)\nabla\phi_j) + (\mathbf{q}(\mathbf{x}_j)\cdot\nabla\phi_j)\phi_i)\, d\Omega - \sum_{k=1}^{n_{be_3}} \int_{\Gamma_3^{e_k}} \sigma\phi_j\phi_i d\Gamma, \tag{3.12}$$

$$\begin{aligned} f_i = &\sum_{k=1}^{n_e} \int_{\Omega^{e_k}} (q_{so}C_s)(\mathbf{x}_j)\phi_i d\Omega + \sum_{k=1}^{n_{be_2}} \int_{\Gamma_2^{e_k}} g_2(\mathbf{x}_j)\phi_i d\Gamma + \sum_{k=1}^{n_{be_3}} \int_{\Gamma_3^{e_k}} g_3(\mathbf{x}_j)\phi_i d\Gamma \\ &- \sum_{k=1}^{n_{be_3}} \int_{\Gamma_3^{e_k}} \sigma \sum_{j=n+1}^{n+n_B} g_1(\mathbf{x}_j)\phi_j\phi_i d\Gamma - \sum_{k=1}^{n_e} \int_{\Omega^{e_k}} \sum_{j=n+1}^{n+n_B} (\nabla\phi_i \cdot (\theta D g_1(\mathbf{x}_j)\nabla\phi_j) \\ &+ (\mathbf{q}\cdot(g_1(\mathbf{x}_j)\nabla\phi_j))\phi_i)\, d\Omega. \end{aligned} \tag{3.13}$$

It is assumed that the boundary of the domain equals the outer boundary of the elements.

Only those basis functions corresponding to nodal points in the element e_k have a non-zero contribution to the integrals for this element. So for a tetrahedron shaped element e_k only a small number of the integrals over the element is unequal to zero. These integrals are computed and stored in an element matrix. For a linear tetrahedron such an element matrix is a 4×4 matrix. The element vector corresponding to q_i reduces to a 4×1 vector.

The elements of the element matrix and element vector are computed with a numerical integration rule. The Newton-Cotes rule is based upon exact integration of the basis functions

$$func(\mathbf{x}) \approx \sum_{k=1}^{d+1} func(\mathbf{x_k})\phi_k(\mathbf{x}), \tag{3.14}$$

with $d+1$ the number of basis functions in the element, and application of the general rule:

Theorem 1

$$\int_{simplex} \phi_1^{m_1}\phi_2^{m_2}...\phi_{d+1}^{m_{d+1}} d\Omega = \frac{m_1!m_2!...m_{d+1}!}{(m_1+m_2+...+m_{d+1}+d)!}|\Delta| \tag{3.15}$$

where d denotes the dimension of space.

Take a linear shaped element or simplex in $\mathbb{R}^3$. From Definition 1 of the linear basis function it follows that for this tetrahedron:

$$\phi_i(\mathbf{x}) = a_0^i + a_1^i x + a_2^i y + a_3^i z, \tag{3.16}$$

and hence

$$\nabla\phi_i \;=\; \begin{bmatrix} a_1^i \\ a_2^i \\ a_3^i \end{bmatrix}. \tag{3.17}$$

From the definition of the basis functions it also follows that $XA = I$ with

$$A = \begin{bmatrix} a_0^1 & a_0^2 & a_0^3 & a_0^4 \\ a_1^1 & a_1^2 & a_1^3 & a_1^4 \\ a_2^1 & a_2^2 & a_2^3 & a_2^4 \\ a_3^1 & a_3^2 & a_3^3 & a_3^4 \end{bmatrix} \quad X = \begin{bmatrix} 1 & x_1 & y_1 & z_1 \\ 1 & x_2 & y_2 & z_2 \\ 1 & x_3 & y_3 & z_3 \\ 1 & x_4 & y_4 & z_4 \end{bmatrix}, \tag{3.18}$$

so $A = X^{-1}$. A necessary condition for the existence of ϕ_i is that the determinant of the matrix X is unequal to zero. The absolute value of this determinant is given by:

$$\begin{aligned} |\Delta| = {} & x_1 \left(-y_3 z_4 + z_3 y_4 + y_2 z_4 - z_2 y_4 - y_2 z_3 + z_2 y_3\right) + \\ & + x_2 \left(y_3 z_4 - z_3 y_4 - y_1 z_4 + z_1 y_4 + y_1 z_3 - z_1 y_3\right) + \\ & + x_3 \left(-y_2 z_4 + z_2 y_4 + y_1 z_4 - z_1 y_4 - y_1 z_2 + z_1 y_2\right) + \\ & + x_4 \left(y_2 z_3 - z_2 y_3 - y_1 z_3 + z_1 y_3 + y_1 z_2 - z_1 y_2\right). \end{aligned} \tag{3.19}$$

The elements of the matrix A can be determined by the calculation of X^{-1}:

$$A = X^{-1} = \frac{adj(X)}{|\Delta|}$$

with $adj(X)$ the adjugate matrix of X. The definition of the adjugate matrix can be found in Section 3.3 of Lay [12].

From (3.14) and (3.15) it follows that the Newton-Cotes rule for the tetrahedron is defined by:

$$\int_{\Omega_{e_k}} f(\mathbf{x}) d\Omega = \frac{|\Delta|}{24} \sum_{l=1}^{4} f(\mathbf{x}_l), \tag{3.20}$$

where $\mathbf{x}_l$ is the l^{th} vertex of the triangle. The Newton-Cotes rule for the boundary element is defined by:

$$\int_{\Gamma_{e_k}} f(\mathbf{x}) d\Gamma = \frac{|\tilde{\Delta}|}{6} \sum_{l=1}^{3} f(\mathbf{x}_l), \tag{3.21}$$

with $|\tilde{\Delta}|$ two times the area of the triangle at the boundary.

Application of the Newton-Cotes rule results in the element matrices and vector (with 1,2,3,4 the vertices of the tetrahedron). The mass-matrix M

$$M^{e_k} = \begin{vmatrix} m_{11}^{e_k} & m_{12}^{e_k} & m_{13}^{e_k} & m_{14}^{e_k} \\ m_{21}^{e_k} & m_{22}^{e_k} & m_{23}^{e_k} & m_{24}^{e_k} \\ m_{31}^{e_k} & m_{32}^{e_k} & m_{33}^{e_k} & m_{34}^{e_k} \\ m_{41}^{e_k} & m_{42}^{e_k} & m_{43}^{e_k} & m_{44}^{e_k} \end{vmatrix}, \tag{3.22}$$

with

$$m_{ij}^{e_k} = \frac{|\Delta|}{24} \sum_{l=1}^{4} \theta(\mathbf{x}_l) \delta_{ij}. \tag{3.23}$$

The stiffness-matrix S

$$S^{e_k} = \begin{vmatrix} s_{11}^{e_k} & s_{12}^{e_k} & s_{13}^{e_k} & s_{14}^{e_k} \\ s_{21}^{e_k} & s_{22}^{e_k} & s_{23}^{e_k} & s_{24}^{e_k} \\ s_{31}^{e_k} & s_{32}^{e_k} & s_{33}^{e_k} & s_{34}^{e_k} \\ s_{41}^{e_k} & s_{42}^{e_k} & s_{43}^{e_k} & s_{44}^{e_k} \end{vmatrix}, \tag{3.24}$$

with

$$s_{ij}^{e_k} = -\frac{|\Delta|}{24}\sum_{l=1}^{4}(\nabla\phi_i \cdot \theta(\mathbf{x}_l)D(\mathbf{x}_l)\nabla\phi_j + (\mathbf{q}(\mathbf{x}_l)\cdot\nabla\phi_j)\phi_i) - \frac{|\tilde{\Delta}|}{6}\sum_{l=1}^{3}\sigma(\mathbf{x}_l)\delta_{ij}, \tag{3.25}$$

or

$$s_{ij}^{e_k} = -\frac{|\Delta|}{24}\left((\nabla\phi_i\cdot\nabla\phi_j)\sum_{l=1}^{4}(\theta(\mathbf{x}_l)D(\mathbf{x}_l)) + \nabla\phi_j\cdot\sum_{l=1}^{4}\mathbf{q}(\mathbf{x}_l)\delta_{il}\right) - \frac{|\tilde{\Delta}|}{6}\sum_{l=1}^{3}\sigma(\mathbf{x}_l)\delta_{ij}, \tag{3.26}$$

and

$$f_i^{e_k} = \begin{vmatrix} f_1^{e_k} \\ f_2^{e_k} \\ f_3^{e_k} \\ f_4^{e_k} \end{vmatrix}, \tag{3.27}$$

with

$$\begin{aligned} f_i^{e_k} = {} & \frac{|\Delta|}{24}\sum_{l=1}^{4}q_{so}(\mathbf{x}_l)C_s(\mathbf{x}_l)\delta_{il} + \frac{|\tilde{\Delta}|}{6}\sum_{l=1}^{3}g_2(\mathbf{x}_l)\delta_{il} + \frac{|\tilde{\Delta}|}{6}\sum_{l=1}^{3}g_3(\mathbf{x}_l)\delta_{il} \\ & - \frac{|\Delta|}{24}\sum_{l=1}^{4}\sum_{j=n+1}^{n+n_B}(\nabla\phi_i\cdot(\theta(\mathbf{x}_l)D(\mathbf{x}_l)(g_1(\mathbf{x}_l)\nabla\phi_j)) - (\mathbf{q}(\mathbf{x}_l)\cdot g_1(\mathbf{x}_l)\nabla\phi_j)\delta_{il}) \\ & - \frac{|\tilde{\Delta}|}{6}\sum_{l=1}^{3}\sigma(\mathbf{x}_l)\sum_{j=n+1}^{n+n_B}g_1(\mathbf{x}_l)\delta_{ij}. \end{aligned} \tag{3.28}$$

Remark: if Newton-Cotes integration is applied for the coefficients of the mass matrix, then the mass matrix reduces to a diagonal matrix. In that case M is called a lumped mass matrix. A non-lumped matrix is also known as a consistent mass matrix and might have a better accuracy for advection dominated problems. This difference in accuracy is determined by a constant, not by an order and is experimentally discovered, not proved.

Spatial discretization: SUPG

According to [9] it can be shown that the Standard Galerkin Approach in combination with the FEM yields an accuracy of $O(h^{k+1})$, where h is some representative diameter of the tetrahedrons and k is the degree of the polynomials used in the aproximation per element. However, this is only true for problems, where advection does not dominate dispersion. As soon as the advection dominates, the accuracy strongly deteriorates. Inspired by upwind finite differences, upwind finite elements have been developed to preclude wiggles. These upwind methods can represent a significant improvement over the Standard Galerkin Approach, but problems have been noted with the treatment of source terms, time dependent behavior and with the generalization to multidimensions. In these cases, pronounced dispersion corrupts the true solution. For more information about these techniques and their problems, see [13].

An example of a class of upwind methods is the class of Petrov-Galerkin methods (PG), that can be used in order to obtain a better accuracy and less

wiggles for advection dominated flows. The results of the accuracy of both methods can be found in Chapter 5. PG methods are methods in which the test functions and the basis functions for the solution have different shapes. Split the testfunction $\eta(\mathbf{x})$ into two parts :

$$\eta(\mathbf{x}) = w(\mathbf{x}) + b(\mathbf{x}), \tag{3.29}$$

where $w(\mathbf{x})$ is the classical test function from the same function space as the solution and $b(\mathbf{x})$ is used to take care of the upwind behavior. The $w(\mathbf{x})$ part ensures the consistency of the scheme. This function must be so smooth that integration by parts is allowed. The function $b(\mathbf{x})$ on the other hand will be defined elementwise, which means that it may be discontinuous over the element boundaries. Rewrite the weak formulation before the application of Green's theorem (Equation (3.3)) by substitution of (3.29):

$$\int_\Omega \left\{ -\nabla \cdot (\theta D \nabla C) + \mathbf{q} \cdot \nabla C + \theta \frac{\partial C}{\partial t} - q_{so} C_s \right\} (w + b) d\Omega = 0. \tag{3.30}$$

The function $b(\mathbf{x})$ can be discontinuous over the elements, hence Green's theorem (see 3.4) can only be applied to the $w(\mathbf{x})$ part of (3.30). After the application of this theorem, Equation (3.30) becomes:

$$\begin{aligned} &\int_\Omega \left((\nabla w) \cdot (\theta D \nabla C) + (\mathbf{q} \cdot \nabla C) w + \theta \frac{\partial C}{\partial t} w \right) d\Omega + \int_{\Gamma_3} \sigma C w d\Gamma + \\ &\quad + \int_\Omega \left\{ -\nabla \cdot (\theta D \nabla C) + \mathbf{q} \cdot \nabla C + \theta \frac{\partial C}{\partial t} - q_{so} C_s \right\} b d\Omega = \\ &\quad = \int_\Omega q_{so} C_s w d\Omega + \int_{\Gamma_2} g_2 w d\Gamma + \int_{\Gamma_3} g_3 w d\Gamma. \end{aligned} \tag{3.31}$$

It is possible that $\nabla \cdot (\theta D \nabla C)$ does not exist over the element boundaries and that the integral containing the b term can only be computed by a summation over the elements. In order to solve this problem the integral containing b is splitted into a sum of integrals over the elements, and the inter-element contributions are neglected. Reformulation of Equation (3.31) results in:

$$\begin{aligned} &\int_\Omega \left((\nabla w) \cdot (\theta D \nabla C) + (\mathbf{q} \cdot \nabla C) w + \theta \frac{\partial C}{\partial t} w \right) d\Omega + \int_{\Gamma_3} \sigma C w d\Gamma + \\ &\quad + \sum_{k=1}^{n_e} \int_{\Omega^{e_k}} \left\{ -\nabla \cdot (\theta D \nabla C) + \mathbf{q} \cdot \nabla C + \theta \frac{\partial C}{\partial t} \right\} b d\Omega = \\ &\quad = \int_\Omega q_{so} C_s w d\Omega + \int_{\Gamma_2} g_2 w d\Gamma + \int_{\Gamma_3} g_3 w d\Gamma + \\ &\quad + \sum_{k=1}^{n_e} \int_{\Omega^{e_k}} q_{so} C_s b d\Omega. \end{aligned} \tag{3.32}$$

Note that the basis functions are linear, hence the term $-\nabla \cdot (\theta D \nabla C) = -\nabla C \cdot \nabla \theta D$ per element.

The choice of the function $b(\mathbf{x})$ is completely free but actually defines the type of the PG method.

Brooks and Hughes [13] tried to apply upwind only in the direction of the velocity of the flow of a more dimensional problem. They achieved this by giving the perturbation parameter b a tensor character:

$$b(\mathbf{x}\ ) = \frac{|\tilde{\Delta}|\xi}{2}\frac{\nabla\phi_i \cdot \mathbf{q}}{||\mathbf{q}||},$$

with $\frac{\nabla\phi_i \cdot \mathbf{q}}{||\mathbf{q}||}$ the inner product of the gradient of the basis function and the direction of the velocity and $|\tilde{\Delta}|$ some representative distance in the element, preferably in the direction of $\mathbf{q}$. This choice of $b(\mathbf{x})$ is called the Streamline Upwind Petrov Galerkin method (SUPG), since streamlines (lines which are everywhere tangent to the velocity of the flow) are always in the direction of the velocity. The explanation in two dimensions is given. Call $\Psi = constant$ a streamline, ϕ the potential and q_x the x-component of the velocity vector $\mathbf{q}$. By definition, $q_x = \frac{\partial\phi}{\partial x}$ and $q_y = \frac{\partial\phi}{\partial y}$. Also by definition, $q_x = \frac{\partial\Psi}{\partial y}$ and $q_y = -\frac{\partial\Psi}{\partial x}$. Hence

$$\nabla\Psi = \begin{bmatrix} \frac{\partial\Psi}{\partial x} \\ \frac{\partial\Psi}{\partial y} \end{bmatrix} = \begin{bmatrix} -q_y \\ q_x \end{bmatrix}.$$

The inner product $(\nabla\Psi, \nabla\phi) = 0$. So if $\Psi = constant$, ϕ perpendicular to Ψ is also constant. The conclusion is that $\Psi = constant$ is the direction of the velocity.

For a three dimensional problem, $|\tilde{\Delta}|$ equals two times the area of the triangular at the boundary. The following values of ξ are commonly proposed;

Classical upwind scheme

$$\xi = sign(\alpha), \tag{3.33}$$

Il'in scheme

$$\xi = coth(\alpha) - 1/\alpha, \tag{3.34}$$

Double asymptotic approximation

$$\xi = \begin{cases} \alpha/3 & -3 \leq \alpha \leq 3, \\ sign(\alpha) & |\alpha| > 3, \end{cases} \tag{3.35}$$

Critical approximation

$$\xi = \begin{cases} -1 - 1/\alpha & \alpha \leq -1, \\ 0 & -1 \leq \alpha \leq 1, \\ 1 - 1/\alpha & \alpha \geq 1, \end{cases} \tag{3.36}$$

In 1D α equals

$$\alpha = \frac{q\Delta x}{2D\theta}. \tag{3.37}$$

For more dimensions α can be taken as

$$\alpha = \frac{\mathbf{q} \cdot \Delta\mathbf{x}}{2D\theta}. \tag{3.38}$$

[9], [6], [13].

Flux-limiter TVD algorithm

Solutions produced by standard discretization techniques are typically corrupted by nonphysical oscillations and/or excessive numerical dispersion. Traditionally, these problems have been dealt with by means of a nonlinear shock-capturing viscosity, like the SUPG methods. Modern high-resolution schemes are based on flux/slope limiters which switch between linear high- and low-order discretizations adaptively depending on the smoothness of the solution.

Definition 1 *For one dimension, a method is called* Total Variation Diminishing (TVD) *if, for any set of data Q^n, the values Q^{n+1} computed by the method satisfy*

$$TV(Q^{n+1}) \leq TV(Q^n), \tag{3.39}$$

with

$$TV(Q^n) = \sum_{i=-\infty}^{\infty} |Q_i^n - Q_{i-1}^n|. \tag{3.40}$$

If a method is TVD, then in particular for data that are initially monotone, say

$$Q_i^n \geq Q_{i+1}^n \qquad \text{for all } i,$$

the method will remain monotone in all future time steps. Hence if a single propagating discontinuity is discretized, the discontinuity may become smeared in future time steps but cannot become oscillatory. A TVD method is monotonicity-preserving. (Proof for two-step method (3 time levels are involved in the scheme)/hyperbolic conservation law/conservative scheme follows or see [14])

Definition 2 *A method is called* monotonicity-preserving *if*

$$Q_i^n \geq Q_{i+1}^n \qquad \textit{for all } i,$$

implies that

$$Q_i^{n+1} \geq Q_{i+1}^{n+1} \qquad \textit{for all } i.$$

This implies that a TVD method is stable. Note that stability plus consistency implies convergence. This is known as Lax's equivalence theorem. The definitions of *consistency*, *stability*, *convergence*, *local truncation error* and *global truncation error* can be found in Appendix B. [15]

The total variation diminishing methods, established by Harten [16], have enjoyed an increasing popularity over the past two decades but have hardly been used in the finite element context. Numerical results were quite promising, but such schemes do not guarantee preservation of positivity, may fail to suppress the nonphysical oscillations in some cases and this approach is not suitable for multilinear (mathematical function of several vector variables that is linear in each variable) and higher order finite elements.

Consider again the three dimensional advection-dispersion Equation (2.17)

$$\theta \frac{\partial C}{\partial t} + \nabla \cdot (-\theta D \nabla C + \mathbf{q}C) = q_{so} C_s, \tag{3.41}$$

Write

$$\mathbf{f} = -\theta D \nabla C + \mathbf{q}C, \tag{3.42}$$

$$\mathbf{f} = \mathbf{f}_c + \mathbf{f}_d,$$

with

$$\mathbf{f}_c = \mathbf{q}C,$$
$$\mathbf{f}_d = -\theta D \nabla C.$$

The weak form can be written as

$$\int_\Omega \theta\eta \frac{\partial C}{\partial t} d\Omega - \int_\Omega \nabla\eta \cdot \mathbf{f} d\Omega + \int_\Gamma \eta \mathbf{f} \cdot \mathbf{n} d\Gamma - \int_\Omega \eta q_{so} C_s d\Omega = 0 \qquad \forall\eta \tag{3.43}$$

Discretization in space is done by the interpolation of the fluxes and source terms in the same way as the numerical solution:

$$C = \textstyle\sum_j C_j \phi_j, \quad \mathbf{f} = \sum_j \mathbf{f}_j \phi_j, \quad q_{so} C_s = \sum_j (q_{so} C_s)_j \phi_j, \tag{3.44}$$

where ϕ_j again denotes the basis functions spanning the finite-dimensional subspace. The Galerkin discretization of equation (3.43) reads:

$$\sum_j \left[\int_\Omega \phi_i \phi_j d\Omega\right] \left(\theta \frac{dC}{dt} - (q_{so} C_s)_j\right) - \sum_j \left[\int_\Omega \nabla\phi_i \phi_j d\Omega - \int_\Gamma \phi_i \phi_j \mathbf{n} d\Gamma\right] \cdot \mathbf{f}_j = 0 \tag{3.45}$$

The Galerkin method possess the global conservation property and can be written as

$$M_L \theta \frac{dC}{dt} = SC + M_L q_{so} C_s. \tag{3.46}$$

Here $M_L = diag\{m_i\}$ denotes the lumped mass matrix (all mass is put in the diagonal elements) with the entries

$$m_i = \sum_j m_{ij}, \quad \text{where} \quad m_{ij} = \int_\Omega \phi_i \phi_j d\Omega \tag{3.47}$$

The discrete transport operator $S = \{s_{ij}\}$ is assembled from [17]

$$s_{ij} = -\mathbf{q}_j \cdot \beta_{ji} - \theta(\mathbf{x}_j) D(\mathbf{x}_j) \gamma_{ij}, \tag{3.48}$$

where β_{ji} and γ_{ij} result from the discretization of differential operators corresponding to the first- and second-order derivatives, respectively

$$\beta_{ji} = \int_\Omega \phi_i \nabla\phi_j d\Omega, \quad \gamma_{ij} = \int_\Omega \nabla\phi_i \cdot \nabla\phi_j d\Omega. \tag{3.49}$$

After lumping, the ODE for each nodal value C_i can be represented in the form

$$m_i \theta_i \frac{dC_i}{dt} = \sum_{j \neq i} s_{ij}(C_j - C_i) + \sum_j s_{ij} C_i + (q_{so} C_s)_i. \tag{3.50}$$

The second term in the right-hand side vanishes for divergence-free velocity fields. For the numerical solution to be nonoscillatory even in the vicinity of steep gradients, all off-diagonal coefficients of S must be nonnegative:
$s_{ij} \geq 0$, $j \neq i$ and $S^{-1} \leq 0$. This condition is necessary to enforce the M-matrix property and make the discretization *Local Extremum Diminishing (LED)* for incompressible flows in the absence of source terms ($q_{so_i} C_{s_i} = 0$).

Definition 3 *The matrix S is called an* M-matrix *if S is nonsingular, $S^{-1} \geq 0$ and $s_{ij} \leq 0$, $i \neq j$, $i, j = 1, ..., n$.*

The term $\sum_j s_{ij} C_i + (q_{so} C_s)_i$ in (3.50) allows for an admissible growth and decay of local extrema due to compressibility and sources/sinks. In order to ensure that the positivity of thermodynamic variables is reproduced by the numerical solution, this term may need to be linearized as proposed by Patankar[verwijzing]. *Local Extremum Diminishing* means that a local maximum cannot increase, and a local minimum cannot decrease.

In [18] is shown that if the discretization is a LED scheme, then the scheme is TVD in arbitrary spatial dimensions. Any discrete transport operator S can be rendered LED, also for the case $q_{so_i} C_{s_i} \neq 0$ and if $\nabla \mathbf{q} \neq 0$, by adding a tensor of artificial dispersion $D_a = \{d_{a_{ij}}\}$ designed so as to eliminate its negative off-diagonal entries. The optimal dispersion coefficients are given by

$$d_{a_{ii}} = -\sum_{k \neq i} d_{a_{ik}}, \qquad d_{a_{ij}} = d_{a_{ji}} = max\{0, -s_{ij}, -s_{ji}\}. \tag{3.51}$$

In order to make this method a upwind method, the stiffness-matrix S is derived in a different way. Write $L = S + D_a$ and note that this matrix equals S in dispersion-dominated cases. Discrete upwinding should be performed edge-by-edge in accordance with the sparsity structure of the finite element matrix. Start with the Galerkin operator $L = S$. Then for each pair of neighboring nodes i and j, the required modification is as follows:

$$\begin{array}{ll} l_{ii} = l_{ii} - d_{ij} & l_{ij} = l_{ij} + d_{ij} \\ l_{ji} = l_{ji} + d_{ij} & l_{jj} = l_{jj} - d_{ij}. \end{array} \tag{3.52}$$

Due to thes transformation, L can be turned into an upper or lower triangular matrix if convection dominates.

The higher order flux-limiter FEM-TVD algorithm is described in [18].

Note: Strongly time-dependent problems call for the use of a consistent mass matrix. See Kuzmin no. 231.

[18]

FEM-FCT scheme

zie no. 231 Kuzmin. Levert dit voordelen op tov FEM-TVD? p.2: 'A complete transition to a computationally efficient edge-based data structure is feasible but not mandatory. Hence, the algorithm to be presented can be readily integrated into an existing finite element code while preserving the conventional element-by-element matrix assembly and data access.'

Temporal discretization

The system of ordinary differential equations has to be discretized in time. A choice has to be made between the one-step and multi-step methods. Here the one-step method is considered, so only information of the preceding time-step is used and not of previous time-steps.

The ω-method is given by:

$$\left(\frac{M}{\Delta t} - \omega S\right) C^{n+1} = \left(\frac{M}{\Delta t} + (1-\omega) S\right) C^n + \left((1-\omega) q^n + \omega q^{n+1}\right). \tag{3.53}$$

M is the mass-matrix as defined in equation (3.8) and S the stiffness-matrix as defined in equation (3.9). In the literature it is common to split the matrix S into a advective and dispersive part. Say $S = \tilde{S_1} + \tilde{S_2}$ with

$$\tilde{s}_{1_{ij}} = -\int_\Omega (\mathbf{q} \cdot \nabla \phi_j)\phi_i d\Omega - \int_{\Gamma_3} \sigma \phi_j \phi_i d\Gamma, \tag{3.54}$$

$$\tilde{s}_{2_{ij}} = -\int_\Omega \nabla \phi_i \cdot (\theta D \nabla \phi_j) d\Omega \tag{3.55}$$

The most common values for ω are:

$\omega = 0$	Forward Euler method;
$\omega = \frac{1}{2}$	Crank-Nicolson method;
$\omega = 1$	Backward Euler method.

The Forward Euler method is an explicit method and is relatively cheap. The disadvantage of this method is that the time-step is restricted in order to get a stable solution. The Forward Euler method is instable for small timesteps and an implicit method should be used. The accuracy of the time-discretization of this method is $O(\Delta t)$.

The Backward Euler method is an implicit method and is unconditionally stable for the convection equation. It has the same accuracy as the Forward Euler method. Errors in time in the initial condition will always be damped with this method.

The most accurate method is the Crank-Nicholson method. This scheme is unconditionally stable and the accuracy of this method is $O(\Delta t^2)$. It does not have the damping property of the Backward Euler method and as a consequence once produced errors in time will always be visible. The Crank-Nicholson scheme can be written as

$$\left(\frac{M}{\tau} - 1/2S\right) C^{n+1} = \left(\frac{M}{\tau} + 1/2S\right) C^n + 1/2 f^n + 1/2 f^{n+1}. \tag{3.56}$$

Another common used option is Backward Euler for the dispersive part and Forward Euler for the advective part. For this method better conditions for the stepsize can be derived in order to avoid wiggles. With S_1 the matrix for the dispersive part and S_2 the matrix for the advective part, this scheme results in

$$\left(\frac{M}{\tau} - S_1\right) C^{n+1} = \left(\frac{M}{\tau} + S_2\right) C^n + f^n. \tag{3.57}$$

In [6] the Lax-Wendroff scheme is discussed which is based on the characteristics. When solutions are smooth this method is suitable for hyperbolic conservation laws. In common cases, it is suitable for parabolic problems as the advection-dispersion equation.

In [15] higher order accurate temporal discretization scheme are presented: the Runge-Kutta Methods. These are multistage one-step methods that generate intermediate values as needed to construct higher-order approximations. A second order accurate temporal discretization method is the Runge-Kutta-2 method. A simple second order explicit two-stage method is often sufficient for use with high-resolution methods as the in Section 3.2 described finite element

method MC limiter. This classical method (known as the method of Heun) for the ordinary differential equation $C_t = \Psi(C)$ takes the form

$$\begin{aligned} C_i^* &= C_i^n + \tau\Psi(C_i^n), \\ C_i^{n+1} &= C_i^n + \tfrac{\tau}{2}\left(\Psi(C_i^n) + \Psi(C_i^*)\right). \end{aligned} \tag{3.58}$$

With $f = 0$ this becomes

$$\begin{aligned} \tfrac{M}{\tau}C_i^* &= \tfrac{M}{\tau}C_i^n + SC_i^n, \\ \tfrac{M}{\tau}C_i^{n+1} &= \tfrac{M}{\tau}C_i^n + \tfrac{1}{2}\left(SC_i^n + SC_i^*\right). \end{aligned} \tag{3.59}$$

[19] The advantage of this scheme is that is extinguishes the error, instead of the Crank-Nicholson Scheme that only bounds the error. This can bee important for handling a dispersion term. The disadvantage is that it costs twice as much as the other methods.

In [9] and [20] second order accurate schemes are presented with higher calculation costs. [6] [9]

3.3 Finite Volumes

3.3.1 Grid

For the Finite Volume Method, the equation for Solute Transport (2.17) is discretized on a square three-dimensional Cartesian grid. For the arrangements of unknows a staggered grid is used, see Figure 3.5. For the readers and writers convenience, the Finite Volume Method is described for a one dimensional problem, which can easily be extended to a three dimensional problem. The one-dimensional grid can be found in Figure 3.6

3.3.2 Solute transport

Consider the solute transport equation in one dimension:

$$\theta\frac{\partial C}{\partial t} + \frac{\partial qC}{\partial x} - \frac{\partial}{\partial x}\left(\theta D\frac{\partial C}{\partial x}\right) = q_{so}C_s, \qquad x \in \Omega = [a,b] \text{ and } t \in [0,T]. \tag{3.60}$$

As described in the Section Boundary and Initial Conditions (Section 2.5), it is recommended to take a natural boundary condition (i.e. Neumann or Robbins boundary condition) for the outflow boundary. So for the outflow boundary a Neumann condition is given and for the inflow boundary a Dirichlet condition is chosen. The boundary and initial conditions are:

$$\begin{cases} C(a,t) = \alpha \\ \frac{\partial C}{\partial x}(b,t) = \beta \\ C(x,0) = C_0(x). \end{cases} \tag{3.61}$$

The domain Ω is subdivided into segments Ω_j, $j = 1, ..., J$ as shown in Figure 3.6. The segments are called cells and the cell-length, denoted by Δx_j for the j^{th}

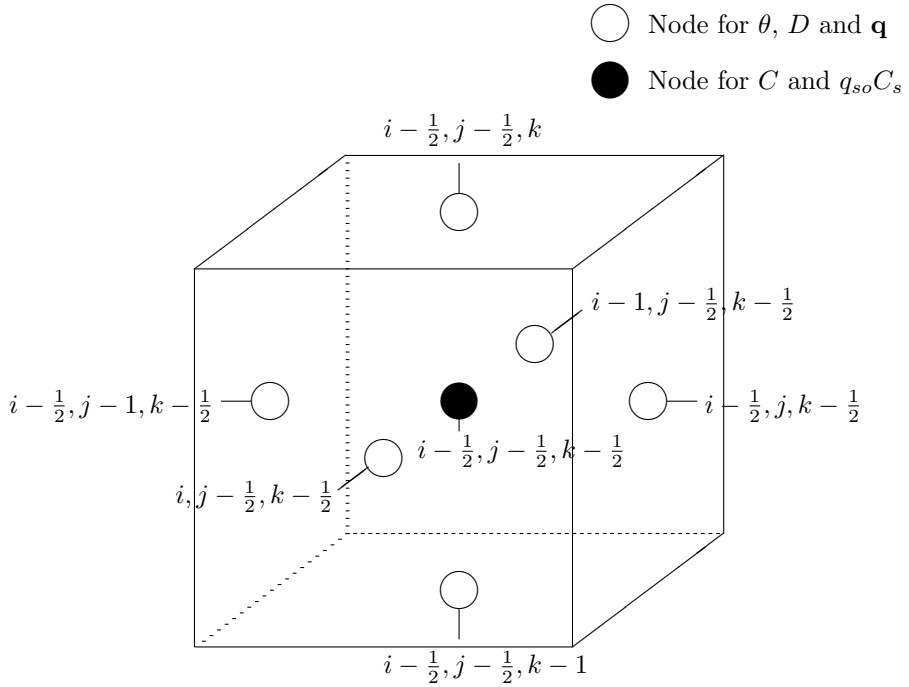

Figure 3.5: One cell of the Cartesian three dimensional staggered grid of the equation for solute transport.

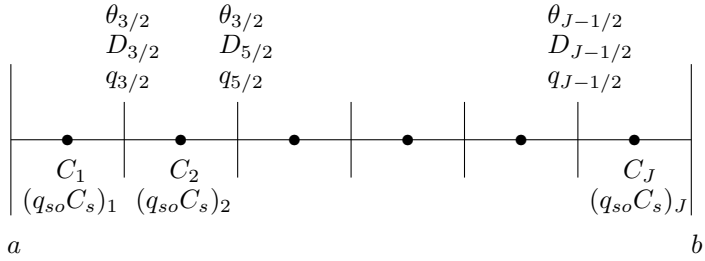

Figure 3.6: The one dimensional Finite Volume grid.

cell, is called the mesh size. Integrate equation (3.60) over Ω_j and approximate this integral by

$$\Delta x_j \theta_j \frac{\partial C}{\partial t} - F|_{j-1/2}^{j+1/2} = \Delta x_j \left(q_{so} C_s\right)_j, \qquad j = 1, ..., J, \tag{3.62}$$

with

$$\begin{aligned} F|_{j-1/2}^{j+1/2} &= F_{j+1/2} - F_{j-1/2}, \\ F_{j+1/2} &= F(x_{j+1/2}), \\ F(x) &= \theta D \frac{\partial C}{\partial x} - qC. \end{aligned} \tag{3.63}$$

F(x) is called the flux, qC the advective flux and $\theta D \frac{\partial C}{\partial x}$ the dispersive flux. Equation (3.62) can be rewritten as

$$\frac{\partial C}{\partial t} + \frac{-F_{j+1/2} + F_{j-1/2}}{\Delta x_j \theta_j} = \frac{\left(q_{so} C_s\right)_j}{\theta_j}. \tag{3.64}$$

Call

$$LC_j = \frac{-F_{j+1/2} + F_{j-1/2}}{\Delta x_j \theta_j}. \tag{3.65}$$

The temporal discretization with the ω-scheme can now be written as

$$\frac{C_j^{n+1} - C_j^n}{\tau} + (1-\omega) LC_j^n + \omega LC_j^{n+1} = \omega \left(\frac{q_{so} C_s}{\theta}\right)_j^{n+1} + (1-\omega) \left(\frac{q_{so} C_s}{\theta}\right)_j^n, \tag{3.66}$$

with τ the time step. Note that θ and D are constant in time and vary only in x; so $\theta_j^n = \theta_j$ and $D_j^n = D_j \ \forall n$. The source term $q_{so} C_s$ and the velocity q depend on time. As mentioned before, it is common to discretize the advective term with Forward Euler and the dispersive term with Backward Euler. Split the flux F into an advective flux $Fa = -qC$ and a dispersive flux $Fd = \theta D \frac{dC}{dx}$. If the dispersive part is temporal discretized with Forward Euler, this parabolic equation is only stable if $\tau = O(\Delta x^2)$. Instead an implicit method is preferable, such as Backward Euler ($\omega = 1$) or the Crank-Nicholson method (ω=1/2).

For the options 1, 2 and 3 Forward Euler discretization is chosen for the advective term and source term and Backward Euler discretization is chosen for the dispersive term. In the options 1, 2 and 3 different numerical methods are studied of the form

$$\begin{aligned} &C_j^{n+1} + \tfrac{\tau}{\Delta x_j \theta_j} \left(-Fd_{j+1/2}^{n+1} + Fd_{j-1/2}^{n+1}\right) = \\ &= C_j^n - \tfrac{\tau}{\Delta x_j \theta_j} \left(-Fa_{j+1/2}^n + Fa_{j-1/2}^n\right) + \left(\tfrac{q_{so} C_s}{\theta}\right)_j^n \end{aligned} \tag{3.67}$$

The flux $F_{j+1/2}$ has to be approximated in terms of neighboring grid functions. For all options, the dispersive part of Equation (3.66) is discretized in space with central differences

$$\begin{aligned} Fd_{j+1/2}^{n+1} &= \left(\theta D \tfrac{dC}{dx}\right)_{j+1/2}^{n+1} \approx (\theta D)_{j+1/2} \left(\tfrac{C_{j+1}^{n+1} - C_j^{n+1}}{\Delta x_{j+1/2}}\right) \\ \Delta x_{j+1/2} &\approx \tfrac{1}{2}(\Delta x_j + \Delta x_{j+1}), \end{aligned} \tag{3.68}$$

For the spatial discretization of the advective flux, different methods are studied.

Option 1
The first option is to investigate Equation (3.67) with the *first order upwind* discretization for the advective flux Fa:

$$Fa^n_{j+1/2} = -\left(qC\right)^n_{j+1/2} \approx -\frac{1}{2}\left(q_{j+1/2} + |q_{j+1/2}|\right) C^n_j - \frac{1}{2}\left(q_{j+1/2} - |q_{j+1/2}|\right) C^n_{j+1}. \tag{3.69}$$

For advective dominated problems it is expected that information about the concentration can be found backwards in space. For a system of equations there might be several waves propagating at different speeds and perhaps in different directions. It makes sense to use the knowledge of the structure of the solution to determine better numerical flux functions. This idea gives rise to *upwind* methods in which the information for the concentration is obtained by looking in the direction from which this information should be coming.

For a scalar advection equation (q constant), there is only one speed, which is either positive or negative. So an upwind method is typically an one-sided method with first order accuracy in space. For the one dimensional advection-dispersion equation the inequality $|\frac{q\tau}{\Delta x}| \leq 1$ must be satisfied in order for this method to be stable. This condition follows also from the CFL-condition.

The CFL condition is a necessary condition that must be satisfied by any finite volume method if stability and convergence to the solution of the differential equation as the grid is refined is expected. Its formal definition is

Definition 1 *The CFL condition is defined as: a numerical method can be convergent only if its numerical domain of dependence contains the true domain of dependence of the PDE, at least in the limit as τ and Δx go to zero.*

In Section 4.4 of Leveque [15] the CFL condition is derived for the one dimensional advection equation with a three-point stencil

$$\mu \equiv |\frac{q\tau}{\Delta x}| \leq 1. \tag{3.70}$$

This condition holds also for the advection-dispersion equation.

Option 2
To obtain a second-order accurate discretization in space for the advective part, a *high-resolution method with nonzero slope* is used as derived in [15]. A nonzero slope is chosen in such a way that the slope approximates the derivative over the ith cell.

Assume the velocity $q > 0$ and $|q\tau/\Delta x| \leq 1$ as is required by the CFL condition, then the advective flux in Equation (3.69) can be written as

$$Fa^n_{j+1/2} = -\left(qC\right)^n_{j+1/2} \approx -q_{j+1/2} C^n_j.$$

With a nonzero slope the advective flux becomes

$$Fa^n_{j+1/2} = -q_{j+1/2} C^n_j - \frac{1}{2} q_{j+1/2}(\Delta x - q_{j+1/2}\tau)\sigma^n_j. \tag{3.71}$$

Three possibilities for the nonzero slope are:

$$\text{Centered slope:} \qquad \sigma^n_j = \frac{C^n_{j+1} - C^n_{j-1}}{2\Delta x_j} \qquad \text{(Fromm)}, \tag{3.72}$$

$$\text{Upwind slope:} \qquad \sigma_j^n = \frac{C_j^n - C_{j-1}^n}{\Delta x_j} \qquad \text{(Beam-Warming)}, \tag{3.73}$$

$$\text{Downwind slope:} \qquad \sigma_j^n = \frac{C_{j+1}^n - C_j^n}{\Delta x_j} \qquad \text{(Lax-Wendroff)}, \tag{3.74}$$

Option 3
Second-order accurate methods such as Lax-Wendroff or Beam-Warming give much better accuracy on smooth solutions than the upwind method, but fail near discontinuities, where oscillations are generated. In fact for the advective equation, according to [15], even when the solution is smooth, oscillations may appear due to the dispersive nature of these methods. Upwind methods have the advantage that they cannot introduce oscillations, so they keep the solution monotonically varying in regions where the solution should be monotone. The disadvantage on the other hand is that they smear the solution.

In *option 3* high-resolution methods are presented that combine the best features of both the upwind and the second-order accurate methods. Second-order accuracy is obtained where possible, but it is not insisted in regions where the solution is not behaving smoothly. The idea is to apply some form of limiter that changes the magnitude of the correction actually used, depending on how the solution is behaving. This leads to the so-called slope-limiter methods.

Recall the definition for TVD (Definition 1 in Section 3.2.3). This definition can also be used for the Finite Volume Method. The advantages of a TVD-method are already explained in Section 3.2.3.

The first order upwind method in *option 1* is TVD for the advection equation and has the advantage that it cannot introduce oscillations but the disadvantage that it smears the solution. The methods of *option 2* are not unconditionally TVD methods.

Take again the numerical scheme of Equation (3.67) with the advective flux as described in Equation (3.71). One choice of slope that gives second-order accuracy for smooth solutions while still satisfying the TVD property is the *minmod slope*, which is a slope-limiter method

$$\sigma_j^n = minmod\left(\frac{C_j^n - C_{j-1}^n}{\Delta x}, \frac{C_{j+1}^n - C_j^n}{\Delta x}\right), \tag{3.75}$$

where the minmod function of two arguments is defined by

$$minmod(a,b) = \begin{cases} a & \text{if } |a| < |b| \text{ and } ab > 0, \\ b & \text{if } |b| < |a| \text{ and } ab > 0, \\ 0 & \text{if } ab \leq 0. \end{cases} \tag{3.76}$$

Another popular choice is the *monotonized central-difference limiter* (MC limiter)

$$\sigma_j^n = minmod\left(\left(\frac{C_{j+1}^n - C_{j-1}^n}{2\Delta x_j}\right), 2\left(\frac{C_j^n - C_{j-1}^n}{\Delta x_j}\right), 2\left(\frac{C_{j+1}^n - C_j^n}{\Delta x_j}\right)\right), \tag{3.77}$$

where the midmod function of three arguments is defined by

$$minmod(a,b,c) = minmod(a, minmod(b,c)) \tag{3.78}$$

This compares the central difference of Fromm's method with twice the one-sided slope to either side. In smooth regions this reduces to the centered slope of Fromm's method.

Option 4
In order to obtain a completely second order accurate scheme in time and place, the Crank-Nicholson scheme is used for the temporal discretization (Equation (3.66) with $\omega = 1/2$), central differences are used for the discretization in place for the dispersive flux and the minmod slope of Equation (3.75) is used for the discretization of the advective flux.

---

p 194 Leveque: TVD Time Stepping

3.4 Finite Differences

3.4.1 Grid

The equation for Solute Transport (2.17) is discretized on a square three-dimensional Cartesian grid. For the arrangements of unknows the staggered grid as shown in Section 3.3. For the three dimensional cell and arrangement of unknowns and knowns see Figure 3.6. For the one dimensional Finite Difference grid, see Figure 3.5. Another option is to define the grid lines parallel and perpendicular to the flow lines. This may increase the accuracy but makes it difficult to write the discretized equation in the common used x, y and z coordinate system which are used in most software packages.

3.4.2 Solute transport

The one dimensional advection dispersion equation is given by

$$\theta \frac{\partial C}{\partial t} = \frac{\partial}{\partial x}\left(\theta D \frac{\partial C}{\partial x}\right) - q\frac{\partial C}{\partial x} + q_{so}C_s. \tag{3.79}$$

This can be rewritten as

$$\theta \frac{\partial C}{\partial t} = \theta D \frac{\partial^2 C}{\partial x^2} + \frac{\partial C}{\partial x}\left(\theta \frac{\partial D}{\partial x} + D\frac{\partial \theta}{\partial x}\right) - q\frac{\partial C}{\partial x} + q_{so}C_s. \tag{3.80}$$

Spatial discretisation of Equation (3.80) with central differences for the dispersion terms and upwind differences for the advective terms gives:

$$\begin{aligned}\theta_i \frac{dC}{dt} = {} & \theta_i D_i \frac{C_{i+1} - 2C_i + C_{i-1}}{(\Delta x)^2} + \\ & \frac{C_{i+1} - C_{i-1}}{2\Delta x}\left(\theta_i \frac{D_{i+1/2} - D_{i-1/2}}{\Delta x} + D_i \frac{\theta_{i+1/2} - \theta_{i-1/2}}{\Delta x}\right) \\ & - \frac{1}{2\Delta x}\left(\frac{1}{2}(q_i + |q_i|)C_i + \frac{1}{2}(q_i - |q_i|)C_{i+2}\right) + \\ & \frac{1}{2\Delta x}\left(\frac{1}{2}(q_i + |q_i|)C_{i-2} + \frac{1}{2}(q_i - |q_i|)C_i\right) + q_{so}C_s,\end{aligned} \tag{3.81}$$

with

$$q_i = \frac{q_{i+1/2} + q_{i-1/2}}{2}; \qquad \theta_i = \frac{\theta_{i+1/2} + \theta_{i-1/2}}{2}; \qquad D_i = \frac{D_{i+1/2} + D_{i-1/2}}{2}.$$

Equation (3.81) can be written in the form

$$M\frac{dC}{dt} = SC + q.$$

The temporal discretization is given by the ω-method:

$$\left(\frac{M}{\Delta t} - \omega S\right) C^{n+1} = \left(\frac{M}{\Delta t} + (1-\omega)S\right) C^n + \ (1-\omega)q_{so}^n C_s^n + \omega q_{so}^{n+1} C_s^{n+1}. \tag{3.82}$$

with

$\theta = 0$ Forward Euler method
$\theta = \frac{1}{2}$ Crank-Nicolson method The matrix S can again be split into a matrix for the advection part and for the dispersion part. The matrices M, S_1, S_2 can be found in Appendix G.
$\theta = 1$ Backward Euler method

Upwind discretization is used when the condition for diagonal dominance of the matrix A, ($|a_{ii}| \geq \Sigma_{j=1,j\neq i}^{n} |a_{ij}| \ \forall i = 1, ..., n$), leads to very small grid sizes. The matrix A has to satisfy the condition of diagonal dominance in order to derive a monotone solution.
!Duidelijker opschrijven!
Note that the dispersion coefficients are dependent on the direction of the flow, hence upwind discretization might be better when the requirement of diagonal dominance is only satisfied for very small step sizes. On the other hand, the dispersion coefficient is very small compared to the advection terms so upwind discretization might not change the solution.

3.5 Stability and Artificial dispersion

For the stationary 1D advection dispersion equation the condition $|p_h| \leq 1$ is needed to have a monotone solution. p_h is called the *mesh Péclet number* and is defined as

$$p_h \equiv \frac{Pe\Delta x}{2\theta} \equiv \frac{q\Delta x}{2\theta D}. \tag{3.83}$$

Pe is called the Péclet number and is a measure for by how much the advection dominates the dispersion.

For the instationary advection dispersion equation another method is needed that can give an stability condition.

3.5.1 Amplification factors

Have a look at the spatial discretized advection dispersion equation of the form $M\frac{dC}{dt} = SC + f$ with M the mass matrix, S the stiffness matrix and f the source term. Each numerical procedure has an amplification matrix G which is given by the numerical solution of the error equation $\frac{d\epsilon}{dt} = M^{-1}S\epsilon$:

$$\epsilon^{n+1} = G(\tau M^{-1}S)\epsilon^n. \tag{3.84}$$

A numerical solution method is absolutely stable if for the eigenvalues μ_k of $G(\tau M^{-1}S)$ holds $|\mu_k| < 1$. If the error equation consists of one equation only, i.e. $\epsilon' = \lambda\epsilon$, then the amplification of the numerical solution is referred to as the amplification factor, which is denoted by $V(\tau\lambda)$. The eigenvalues μ_k of $G(\tau M^{-1}S)$ are obtained by substitution of the eigenvalues λ_k of the matrix $M^{-1}S$ into the amplification factor

$$\mu_k = V(\tau\lambda_k).$$

Hence for stability we need

$$|V(\tau\lambda_k)| < 1. \tag{3.85}$$

Note that all eigenvalues λ_k are real-valued and negative ($\lambda < 0$) when S is negative definite and M is positive definite (see Section 10.5 [6]). The amplification matrix for the $\omega-$method is:

$$G(\tau M^{-1}S) = \left(I - \omega\tau M^{-1}S\right)^{-1}\left(I + (1-\omega)\tau M^{-1}S\right).$$

With this theory it is hard to derive a stability condition for methods that solve the equation $M\frac{dC}{dt} = SC + f$ because the eigenvalues of the matrix $M^{-1}S$ have to be calculated. Though it can be used to say something about the boundedness of the error. For Forward Euler, $\omega = 0$:

$$|V(\tau\lambda)| = |1 + \tau\lambda| \to \infty \text{ as } |\lambda| \to \infty.$$

The interval for stability for Forward Euler can be calculated by using Equation (3.85):

$$\tau|\lambda| \leq 2 \tag{3.86}$$

For Backward Euler

$$|V(\tau\lambda)| = |\frac{1}{1-\tau\lambda}| \to 0 \text{ as } |\lambda| \to \infty,$$

and the interval for stability is unbounded:

$$\lambda \in (-\infty, 0) \tag{3.87}$$

and for Crank-Nicholson, $\omega = 1/2$, the amplification factor is

$$|V(\tau\lambda)| = |\frac{1 + \frac{\tau\lambda}{2}}{1 - \frac{\tau\lambda}{2}}| \to 1 \text{ as } |\lambda| \to \infty.$$

and the interval for stability of this explicit method is again (3.87). For the Modified Euler method (Runge-Kutta-2) the amplification factor is given by

$$|V(\tau\lambda)| = |1 + \tau\lambda + \frac{1}{2}(\tau\lambda)^2|,$$

and the interval for stability is given by

$$\tau|\lambda| \leq 1 + \sqrt{5}. \tag{3.88}$$

So for Forward Euler the error does not extinguish and can become large outside the small interval for stability. Backward Euler and Crank-Nicholson are unconditionally stable, but only for Backward Euler the error extinguishes. For Crank-Nicholson the error of the previous time steps is bounded but does not extinguish. The Runge-Kutta-2 scheme has a stability condition that is better than the stablity condition for Forward Euler. [6]

3.5.2 Stability temporal discretization scheme

As an alternative method to estimate the eigenvalues of the matrix $M^{-1}S$, Von Neumann analysis can be used. More information can be found in Chapter 8 in [15] of in Chapter 4 in [21]. In [21] are for the advection-dispersion equation with the $\omega-$scheme the following results obtained: unconditional stability for $1/2 \leq \omega \leq 1$. So the Backward Euler and Crank-Nicholson schemes are unconditionally stable.

For $\omega = 0$ in the $\omega-$scheme (Forward Euler) the necessary and sufficient stability condition according to [21] is:

$$2D\tau \left(\frac{1}{\Delta x^2} \right) \leq 1 \text{ and } \frac{\tau}{2D} \left(\frac{q^2}{1 + |q|\Delta x} \right) \leq 1 \tag{3.89}$$

For the advection equation spatial discretized with the first order upwind method with positive velocity q and temporal discretized with Forward Euler, the Von Neumann stability analysis results in the stability condition:

$$0 \leq \frac{q\tau}{\Delta x} \leq 1. \tag{3.90}$$

The derivation can be found in Chapter 8 of Leveque [15]. $\frac{q\tau}{\Delta x}$ is known as the Courant number. The same condition is derived in Section 12.3 [6] for the 1D advection equation discretized with Forward Euler and central differences.

For the 1D dispersion equation according to [21] the time step after discretization with Forward Euler must satisfy

$$\tau \leq \frac{\Delta x^2}{2D} \tag{3.91}$$

This is the reason why explicit methods are less suitable for the dispersion part of the advection dispersion equation.

Temporal discretization with Forward Euler for the advective part and Backward Euler for the dispersive part results in the condition $|q\tau/dx| \leq 1$, because the dispersive part discretized with Backward Euler is unconditionally stable.

For the Runge-Kutta-2 method the stability conditions are:

$$|\frac{q\tau}{\Delta x}| \leq 1, \qquad \frac{D\tau}{\Delta x^2} \leq \frac{1}{2}. \tag{3.92}$$

3.5.3 TVD methods

For nonlinear numerical methods, like the high resolution method MC-limiter of the finite volume method a different approach for stability must be adopted. The total variation (TV) introduced in Section 3.2 turns out to be an effective tool for studying stability of nonlinear problems. In Section 8.3.5 in Leveque [15] it can be seen that the high resolution TVD method MC limiter is convergent for the advection equation provided the CFL condition is satisfied:

$$|\frac{q\tau}{\Delta x}| \leq 1. \tag{3.93}$$

The methods Fromm (3.72), Beam-Warming (3.73) and Lax-Wendroff (3.74) are not TVD methods and hence not necessary monotonicity preserving (see Section 6.7 [15]). The first order upwind FVM is TVD for the advection equation, so this method for this equation cannot introduce oscillations.

3.6 Accuracy

Three different temporal discretizations are used:

Definition 1 *$T1$ is the temporal discretization that refers to the use of Backward Euler for the dispersion part and Forward Euler for the advection part and the source term. See Equation (3.57).*

Definition 2 *$T2$ is the temporal discretization that refers to the use of the Crank-Nicolson scheme. See Equation (3.53).*

Definition 3 *$T3$ is the temporal discretization that refers to the use of the Runge Kutta 2 scheme. See Equation (3.59).*

The $\omega-$scheme is only second order accurate ($O(\tau^2)$) for $\omega = 1/2$ or $\omega = 1/2 + O(\tau)$ (according to [21]). $T1$ is first order accurate. The schemes $T2$ and $T3$ are second order accurate.

In Section 10.3 of [6] it is demonstrated that the truncation error of the spatial discretization, of the system of ordinary differential equations, causes an error of the same order for the time dependent partial differential equation.

The advection dispersion equation is a second order differential equation (say $2m = 2$, so $m = 1$). In Section 8.6 [6] is shown that it is necessary to estimate the interpolation error for the FEM. Suppose an approximation by k^{th} degree polynomials is used for the FEM. It can be proved that under certain (geometrical) conditions, the error in the L^2-norm is of the order Δx^{k+1}. In general, for each derivative, the interpolation error is reduced by an order 1. So the interpolation error in the L^2-norm is of order Δx^{k+1-m}. Hence for linear shaped basisfunctions the interpolation error for the advection dispersion equation is $O(\Delta x)$. It can be concluded that the finite element methods Standard Galerkin Approach (SGA) and SUPG are first order methods. One of the mentioned (geometrical) conditions is that for a 2D problem, all angels must be smaller than 135^0.

The accuracy of the finite volume methods is shown and proved in [15]. The local truncation error of the first order upwind method is $O(\Delta x)$. The methods Fromm (3.72), Beam-Warming (3.73), Lax-Wendroff (3.74) and MC-limiter (3.77) are second-order accurate ($O(\Delta x^2)$).

The first order finite difference method is $O(\Delta x)$.

3.7 Work

A time step with an implicit scheme requires much more computing work than an explicit scheme. So the timestep of the $\omega-$scheme is cheap for $w = 0$. Runge-Kutta-2 is an explicit method, hence it is not necessary to solve an system of equations.

A higher order method like the MC limiter requires more work in each time step than a first order method.

3.8 Other characteristics

There are four advantages of the finite element grid. First, the triangles of the finite element grid are more suitable for complex areas. Second, in case of grid refinement the error stays small because in the FEM an integration is taken over the element instead of an evaluation of the concentration in one point as in the FVM. The third advantage of the FEM is that it is easier to compute distributed ('parallel rekenen'). The fourth advantage has to due with the method already used in Triwaco to solve the groundwater flow equation, which uses triangular shaped elements in de discretization grid.

The advantage of the finite volume method is the existence of higher order upwind methods which are, at least in 1D, relatively simple to use. In more dimensions this will become a smaller advantage.

3.9 Particle Tracking

De methode van de karakteristieken (bv MOC of MT3D gebruiken dit) maakt gebruik van stroomlijnen. Hiermee is advectie redelijk te modelleren, dispersie gedeelte geeft dan echter problemen. SUPG en andere upwind methoden maken in principe ook gebruik van stroomlijnen. Uitzoeken of deze methode eventueel een verbetering kan opleveren.

3.10 Analytical Solution Methods

The Improved Finite Analytic Laplace Transform Method (IFALT), developed by Lowry and Li [22], is based on the improved finite analytic solution method in space developed by [23] coupled with a Laplace transformation in time.

First the Laplace Transform method (LT) is used to analytically eliminate the time derivative from the time-dependent advection dispersion equation. A steady-state advection dispersion equation is formed in the complex Laplace space. This steady-state equation can be solved using any steady-state spatial solver. For instance, the work by Sudicky [24], [25], [26] is based on a finite element method in space and the LT method in time. This produces a method that is accurate in time, but not in space, since FEM are susceptible to spurious oscillations at high Péclet numbers and can only increase accuracy at considerable computational costs. The IFALT method uses the Improved Finite Analytic method (IFA) to solve the steady-state equation. Finally, the resulting solution is then inverted from Laplace space back to the real space time domain.

Again consider the one dimensional advection dispersion equation:

$$\theta(x)\frac{\partial C}{\partial t} + q(x)\frac{\partial C}{\partial x} - \frac{\partial}{\partial x}\left(\theta(x)D(x)\frac{\partial C}{\partial x}\right) = q_{so}C_s(x), \tag{3.94}$$

with the general boundary condition

$$a + bC + g\left(\theta D\frac{\partial C}{\partial x}\right) = f(t),$$

where a, b, g and $f(t)$ are coefficients or functions that are dependent on the type of boundary condition being modeled. Note that q, D, θ and $q_{so}C_s$ only

depend on x and not on t because the dependence of these parameters must be linear in t. The Laplace transform L of a function $h(t)$ is defined as:

$$L\left[h(t)\right] = \tilde{h}(p) = \int_0^\infty h(t)e^{-pt}dt, \tag{3.95}$$

where $\tilde{h}$ is the transform of h and p is the Laplace transform parameter that is generally complex-valued. Applying this to Equation (3.94) gives

$$q(x)\frac{d\tilde{C}}{dx} - \frac{d}{dx}\left(\theta(x)D(x)\frac{d\tilde{C}}{dx}\right) = -\theta p\tilde{C} + q_{so}C_s(x) + \theta g(x), \tag{3.96}$$

where $\tilde{C}$ indicates the complex valued Laplace transformed concentration and $g(x)$ is an additional 'source' term that is defined as the real valued initial condition. Note that with partial integration

$$L\left[\theta\frac{\partial C}{\partial t}\right] = \int_0^\infty \theta\frac{\partial C}{\partial t}e^{-pt}dt = -\theta C(0,x) + \theta p\tilde{C} = -\theta g(x) + \theta p\tilde{C}.$$

The complex valued concentration $\tilde{C}$ is a function of x and p. Applying the Laplace transform to the boundary condition gives

$$L\left[a + bC + g\left(\theta D\frac{\partial C}{\partial x}\right)\right] = a + b\tilde{C} + g\left(\theta D\frac{\partial \tilde{C}}{\partial x}\right). \tag{3.97}$$

To solve this steady-state equation, IFA is used. The idea is to represent the modeling domain as a series of homogeneous elements. The velocity can still vary within each cell through the addition of a local particle tracking scheme that traces the solution characteristic back to the local element boundary. The other parameters are assumed constant within a cell.

The dispersion terms are re-written using a finite difference approximation. This approximation is substituted back into the steady-state differential equation. Now a first-order hyperbolic differential equation is left which describes the complex valued concentration within an element as a function of x and p. This equation is then solved analytically within each element using the method of characteristics.

The solutions for each element are linked to the neighboring elements through the element boundary conditions, forming a system of algebraic equations. More details can be found in [22].

The IFALT method utilizes the Laplace inversion algorithm developed by DeHoog et al. [27] due to its performance in the area of discontinuities (sharp concentration fronts), and the fact that the inverse for many values of time can be obtained from one set of Laplace parameter evaluations. The form of this algorithm allows the inversion of one nodal point at a time. The inverse Laplace transform, modified from the general form to specify concentration is given by

$$C(x,t) = \frac{1}{2\pi i}\int_{\alpha-i\infty}^{\alpha+i\infty} d^{pt}\tilde{C}(x,p)dp. \tag{3.98}$$

By manipulating the real and imaginary parts of (3.98), an alternative expression is formed:

$$C(x,t) = \frac{e^{\alpha t}}{\pi}\int_0^\infty \left\{Re\left[\tilde{C}(x,p)\right]cos\omega t - Im\left[\tilde{C}(x,p)\right]sin\omega t\right\}, \tag{3.99}$$

where Re and Im denote the real and imaginary parts of their arguments and α and ω are defined below. Discretization of (3.99) using a trapezoidal rule with a step size of π/T gives:

$$\begin{aligned} C(x,t) \approx \tfrac{e^{\alpha t}}{T} \left\{ \tfrac{1}{2} Re\left[\tilde{C}(x,\alpha)\right] + \textstyle\sum_{k=0}^{2N+1} Re\left[\tilde{C}(x,p)\right] cos\omega t \right. \\ \left. - \textstyle\sum_{k=0}^{2N+1} Im\left[\tilde{C}(x,p)\right] sin\omega t \right\}, \end{aligned} \tag{3.100}$$

where $\omega = i\pi/T$. The infinite series in Equation (3.100) have been truncated to $2N+1$ terms, which introduces an truncation error into the inversion process. From the expression for the error term compared to $(2N+1) \rightarrow \infty$ the parameter α can be evaluated. It is given as

$$\alpha = \mu - ln(E_r)/2T,$$

where μ is the order of $C(x,t)$ such that $|C(x,t)| \leq Me^{\mu t}$ with M being constant. The term E_r is the relative error:

$$E_r = \frac{E}{Me^{\mu t}},$$

and E is an error term that arises since the Fourier coefficients are not exact but are approximations using $\tilde{C}(x,p)$. [22] suggests that $\mu = 0$, $E_r = 10^{-6}$ and $T = 0.8 * t_{max}$ are adequate for most transport problems and recommends using $\alpha = \ln(E')/1.6t_{max}$ where E' is the maximum tolerable relative error and t_{max} is the maximum time of the simulation.

The complete procedure involves calculation $\tilde{C}(x,p_k), [k = 0,1,...,2N]$ for each value of p_k and a single value t_{max}. Once this array is evaluated, inversion at any time $0.1t_{max} < t < t_{max}$ can then be performed. For $t < 0.1t_{max}$, the absolute error becomes unmanageable due to the averaging effect of Fourier series at discontinuities.

The advantages of the IFALT method are the computationally efficiency and the numerically accuracy (low numerical dispersion). There are no Péclet or Courant conditions, it requires no time-stepping and is relatively accurate even at large grid spacing and when applied to advective dominated flow.

There are two types of errors associated with the inversion of the LT, approximation error and truncation error. The first is due to the approximation of the Fourier series.

Chapter 4

Triwaco

4.1 Introduction

The Triwaco package contains a finite element simulation for saturated ground water flow which is called FLAIRS. FLAIRS calculates the groundwater heads and fluxes in a groundwater domain of aquifers and aquitards. The resulting system usually is non-linear due to the boundary flux which depends on the water head. Trace, the accompanying program for streamlines is capable of handling variable density also.

4.2 Grid

FLAIRS calculates the lateral flow in aquifers with a two dimensional finite element method. The 2D grid of the Finite Element Method exists of triangles in the (x, y)-plane with the height in z-direction equal to the height of the aquifer (H_j). Between the aquifers are aquitards with only vertical flow. Communication between aquifers (vertically) is described with the 1D finite difference method. The height of the aquitards (d_j) plus half of the height of the above and underlying aquifers is the length over which the finite difference equations are applied. (see '1 cell of the FD difference grid' in Figure 4.1). Both grids can be found in Figure 4.1.

The finite element grid is generated by the module TESNET. Boundaries and node densities are inputted into TESNET. In addition to these density polygons it is also possible to double the amount of nodes (local grid-refinement) on line elements such as watercourses and fault zones (breuklijnen). It is also possible to choose a node exactly on a source or to choose a grid lines exactly on a fault zone. Around wells so called 'support circles' can be defined, which are used to automatically create a very dense grid around wells.

4.3 Groundwater flow equation

For constant density, the groundwater flow equation in Triwaco is two dimensional. When the density becomes dependent on the location, the height of the

aquifer becomes important. Z, the elevation or height of the aquifer is now introduced which depends on the x and y coordinate. See Figure 4.1.

Darcy's law in terms of the freshwaterhead h_f for a coordinate x_i can be written as:

$$q_i = -k_i \left(\frac{\partial h_f}{\partial x_i} + \frac{\rho - \rho_f}{\rho_f} \frac{\partial z}{\partial x_i} \right). \tag{4.1}$$

With k_i again the freshwater hydraulic conductivity and ρ_f the freshwater density. The Dupuit-assumption allows to express Darcy's law for vertical flow through aquitards and vertically integrated horizontal flow in aquifers. In Figure 2.1 in section 2.1 the numbering of the aquifers and aquitard can be found.

4.3.1 Vertical flow

The vertical flow in Triwaco is solved with the Finite Difference Method. Define

$$k_i = \frac{K_i \rho_f g}{\mu} = \frac{1}{c_i},$$

where g is the acceleration due to gravity, μ is the dynamic viscosity of water and c_j the resistance of aquitard j. The *vertical* flow from aquifer j with freshwater head h_{f_j} at elevation Z_j in the center of the aquifer *through aquitard* $j-1$ with thickness d_{j-1} and vertical intrinsic permeability K_{j-1} to aquifer $j-1$ with

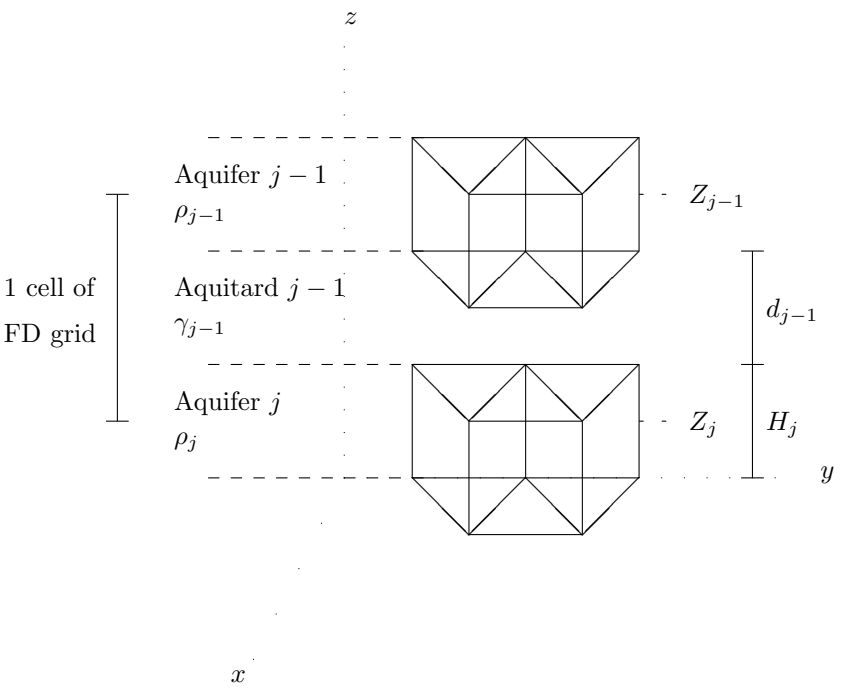

Figure 4.1: 3D grid used in Triwaco. In the aquifers, the horizontal triangles correspond to the finite element grid. Vertically a finite difference grid is used.

freshwater head $h_{f_{j-1}}$ at elevation Z_{j-1} in the center of the aquifer is equal to:

$$\begin{aligned} q_{z,j-1} &= -k_{j-1}\left(\frac{\partial h_f}{\partial x_{j-1}} + \frac{\rho}{\rho_f}\frac{\partial z}{\partial x_{j-1}} - \frac{\partial z}{\partial x_{j-1}}\right). \\ &\cong -k_{j-1}\left(\frac{-h_{f_j} + h_{f_{j-1}}}{d_{j-1}} + \frac{\int_{z=Z}^{Z_{j-1}} \frac{\rho}{\rho_f} dz}{d_{j-1}} + \frac{Z_j - Z_{j-1}}{d_{j-1}}\right), \end{aligned} \tag{4.2}$$

or

$$q_{z,j-1} \cong \frac{h_{f_j} - h_{f_{j-1}} - Z_j + Z_{j-1} - \int_{z=Z_j}^{Z_{j-1}} \frac{\rho}{\rho_f} dz}{c_{j-1}}. \tag{4.3}$$

With c_{j-1} the resistance of aquitard $j-1$. Note that $\frac{\partial h_f}{\partial z} = 0$ within an aquifer because of the hydraulic pressure within an aquifer. The hydraulic pressure is defined as the pressure which is exerted on a portion of a column of fluid as a result of the weight of the fluid above it. So in the application of the finite difference method the used grid size is d_j. More information and the derivation of the integral $\frac{\int_{z=Z_j}^{Z_{j-1}} \frac{\rho}{\rho_f} dz}{d_{j-1}}$ can be found in Olsthoorn [28].

4.3.2 Horizontal flow

Let Q_i denote the horizontal flow in the aquifer ($[L^2T^{-1}]$). The *horizontal* flow *in aquifer* i with thickness H is equal to:

$$\begin{aligned} Q_i &= \int_{z=Z-1/2H}^{Z+1/2H} q_i dz \\ &= \int_{z=Z-1/2H}^{Z+1/2H} \left(-k_i \frac{\partial h_f}{\partial x_i} - k_i \frac{\rho - \rho_f}{\rho_f}\frac{\partial Z}{\partial x_i}\right) dz \\ &= -\kappa_i \int_{z=Z-1/2H}^{Z+1/2H} \frac{\partial h_f}{\partial x_i} dz - -\kappa_i \frac{\partial Z}{\partial x_i} \int_{z=Z-1/2H}^{Z+1/2H} \frac{\rho - \rho_f}{\rho_f} dz, \end{aligned} \tag{4.4}$$

where Z denotes the center of the aquifer and the index $i = 1, 2$ indicates the x and y coordinates.

Remark: In the second step of Equation (4.4) is z replaced by Z without any comment. It is unknown why this is permitted, it might be possible that z in Equation (4.1) must be Z.

Define the transmissivity as $T = kH$ with H the thickness of the aquifer and rewrite Equation (4.4) as:

$$Q_i = -\frac{T_i}{H} \int_{z=Z-1/2H}^{Z+1/2H} \frac{\partial h_f}{\partial x_i} dz - \frac{T_i}{H}\frac{\partial Z}{\partial x_i} \int_{z=Z-1/2H}^{Z+1/2H} \frac{\rho - \rho_f}{\rho} dz. \tag{4.5}$$

With S the storage coefficient and q the sink term, the equation of continuity becomes:

$$\frac{\partial Q_1}{\partial x_1} + \frac{\partial Q_2}{\partial x_2} = q_{z,j} - q_{z,j-1} - S\frac{\partial h_f}{\partial t} - q. \tag{4.6}$$

Substitution of Equation (4.3) and (4.4) in Equation (4.6) results in:

$$\frac{\partial}{\partial x_1}\left(\frac{T_1}{H} \int_{z=Z-1/2H}^{Z+1/2H} \frac{\partial h_f}{\partial x_1} dz\right) + \frac{\partial}{\partial x_2}\left(\frac{T_2}{H} \int_{z=Z-1/2H}^{Z+1/2H} \frac{\partial h_f}{\partial x_2} dz\right) =$$

$$= -\frac{h_{f_{j+1}} - h_f - \int_{z=Z_{j+1}}^{Z} \frac{\rho}{\rho_f} dz}{c_j} - \frac{h_f - h_{f_{j-1}} - \int_{z=Z}^{Z_{j-1}} \frac{\rho}{\rho_f} dz}{c_{j-1}}$$
$$- S\frac{\partial h_f}{\partial t} - q - q^*. \tag{4.7}$$

With q^* the correction flux:

$$q^* = -\frac{\partial}{\partial x_1}\left(\frac{T_1}{H}\frac{\partial Z}{\partial x_1}\int_{z=Z-1/2H}^{Z+1/2H}\frac{\rho-\rho_f}{\rho_f}dz\right) - \frac{\partial}{\partial x_2}\left(\frac{T_2}{H}\frac{\partial Z}{\partial x_2}\int_{z=Z-1/2H}^{Z+1/2H}\frac{\rho-\rho_f}{\rho_f}dz\right) +$$
$$+ \frac{Z_{j+1} - Z - \int_{z=Z_{j+1}}^{Z}\frac{\rho}{\rho_f}dz}{c_j} - \frac{Z - Z_{j-1} - \int_{z=Z}^{Z_{j-1}}\frac{\rho}{\rho_f}dz}{c_{j-1}}. \tag{4.8}$$

First part of 4.7 It has linear shaped functions and numerical calculations based on Galerkin's method. It is assumed that the density is constant in the vertical direction within each aquifer. Equation (4.7) can now be simplified. The density within an aquifer is called ρ, the density in the underlying aquitard is called γ_j and in the above aquitard γ_{j-1}. With d_j the thickness of aquitard j will be denoted and with H_j the thickness of aquifer j, as can be seen in Figure 4.1. The correction flux can be rewritten

$$q^* = -T_1\frac{\partial^2 Z}{\partial x_1^2}\frac{\rho-\rho_f}{\rho_f} - T_1\frac{\partial Z}{\partial x_1}\frac{\partial(\rho/\rho_f)}{\partial x_1} - \frac{\partial T_1}{\partial x_1}\frac{\partial Z}{\partial x_1}\frac{\rho-\rho_f}{\rho_f}$$
$$- T_2\frac{\partial^2 Z}{\partial x_2^2}\frac{\rho-\rho_f}{\rho_f} - T_2\frac{\partial Z}{\partial x_2}\frac{\partial(\rho/\rho_f)}{\partial x_2} - \frac{\partial T_2}{\partial x_2}\frac{\partial Z}{\partial x_2}\frac{\rho-\rho_f}{\rho_f}$$
$$+ \frac{Z_{j+1} - Z + \frac{1}{2}H_{j+1}\frac{\rho_{j+1}}{\rho_f} + d_j\frac{\gamma_j}{\rho_f} + \frac{1}{2}H_j\frac{\rho}{\rho_f}}{c_j}$$
$$- \frac{Z - Z_{j-1} + \frac{1}{2}H\frac{\rho}{\rho_f} + d_{j-1}\frac{\gamma_{j-1}}{\rho_f} + \frac{1}{2}H_{j-1}\frac{\rho_{j-1}}{\rho_f}}{c_{j-1}}. \tag{4.9}$$

4.3.3 FEM for the correction flux

The correction flux of Equation (4.9) is discretized with the Finite Element Method. First, integrate the flux (4.9) over the surface A:

$$Q^* = \int\int_A q^* dx_1 dx_2 \tag{4.10}$$

Split the correction flux into a flux that takes care for the lateral effects within the aquifer Q_l^* and a flux that takes care for the vertical effects to the underlying and above aquifers Q_v^*:

$$Q_l^* = \int\int_A \left\{-T_1\frac{\partial^2 Z}{\partial x_1^2}\frac{\rho-\rho_f}{\rho_f} - T_1\frac{\partial Z}{\partial x_1}\frac{\partial(\rho/\rho_f)}{\partial x_1} - \frac{\partial T_1}{\partial x_1}\frac{\partial Z}{\partial x_1}\frac{\rho-\rho_f}{\rho_f}\right.$$
$$\left. -T_2\frac{\partial^2 Z}{\partial x_2^2}\frac{\rho-\rho_f}{\rho_f} - T_2\frac{\partial Z}{\partial x_2}\frac{\partial(\rho/\rho_f)}{\partial x_2} - \frac{\partial T_2}{\partial x_2}\frac{\partial Z}{\partial x_2}\frac{\rho-\rho_f}{\rho_f}\right\} dx_1 dx_2. \tag{4.11}$$

$$Q_v^* = \int\int_{A_e} \left\{ \frac{Z_{j+1} - Z + \frac{1}{2}H_{j+1}\frac{\rho_{j+1}}{\rho_f} + d_j\frac{\gamma_j}{\rho_f} + \frac{1}{2}H_j\frac{\rho}{\rho_f}}{c_j} - \frac{Z - Z_{j-1} + \frac{1}{2}H\frac{\rho}{\rho_f} + d_{j-1}\frac{\gamma_{j-1}}{\rho_f} + \frac{1}{2}H_{j-1}\frac{\rho_{j-1}}{\rho_f}}{c_{j-1}} \right\} dx_1 dx_2. \quad (4.12)$$

First, the lateral flux is described. Take a triangular shaped element e and assume that the parameters are linear within the element:

$$T_i = T_{i,1}^e x_1 + T_{i,2}^e x_2 + T_{i,0}^e, \quad (4.13)$$

$$Z = Z_1^e x_1 + Z_2^e x_2 + Z_0^e, \quad (4.14)$$

$$\rho = \rho_1^e x_1 + \rho_2^e x_2 + \rho_0^e. \quad (4.15)$$

The second order derivative of Z, $\frac{\partial^2 Z}{\partial x_i^2} = 0$, due to Equation (4.14), so Equation (4.11) simplifies. Call the remaining part the element flux Q_e^*:

$$Q_e^* = -A_e \left\{ T_{1\mu}^e Z_1^e \frac{\rho_1^e}{\rho_f} + T_{1,1}^e Z_1^e \frac{\rho_\mu^e - \rho_f}{\rho_f} + T_{2\mu}^e Z_2^e \frac{\rho_2^e}{\rho_f} + T_{2,2}^e Z_2^e \frac{\rho_\mu^e - \rho_f}{\rho_f} \right\}, \quad (4.16)$$

with μ the mean of the three vertices of the element and A_e the surface of the element. During the linearization of the height Z in Equation (4.14), the second order derivative is neglected. The corresponding term of Equation (4.11) can be important and has to be added:

$$Q_z^* = \int\int_A \left\{ -T_1 \frac{\partial^2 Z}{\partial x_1^2} \frac{\rho - \rho_f}{\rho_f} - -T_2 \frac{\partial^2 Z}{\partial x_2^2} \frac{\rho - \rho_f}{\rho_f} \right\} dx_1 dx_2. \quad (4.17)$$

The flux Q_z^* has to be calculated for each vertex. The number of neighboring vertices has to be determined for each vertex (≥ 2). Dependent on the number and location of the vertices, it is possible to determine 0, 1 or 2 curvatures ('krommingen'). The Laurent- series in the local coordinates ξ and η around the central vertex parallel to x_1 and x_2 as explained in [29] shows the number of curvatures

$$Z \simeq Z_0 + Z_1\xi + Z_2\eta + \frac{1}{2}Z_{11}\xi^2 + Z_{12}\xi\eta + \frac{1}{2}Z_{22}\eta^2, \quad (4.18)$$

where Z_0 is the value of the central vertex, Z_1 and Z_2 are the slopes, Z_{12} the cross-term and Z_{11} and Z_{22} the curvatures: $Z_{ii} = \partial^2 Z/\partial x_i^2$. The definition of the Laurent series can be found in Appendix B. If there are more than five neighboring vertices, the terms can be determined with the Mean Square Error. The Z-curvature flux becomes

$$Q_z^* = -A_n \frac{\rho - \rho_f}{\rho_f} \left\{ T_1 Z_{11} + T_2 Z_{22} \right\}. \quad (4.19)$$

And the lateral flux becomes

$$Q_l^* = \sum \left(\frac{1}{3} Q_e^* \right) + Q_z^*. \quad (4.20)$$

The vertical correction flux (4.12) can be calculated for each vertex:

$$Q_v^* = A_n \left\{ \frac{Z_{j+1} - Z + \frac{1}{2}H_{j+1}\frac{\rho_{j+1}}{\rho_f} + d_j\frac{\gamma_j}{\rho_f} + \frac{1}{2}H_j\frac{\rho}{\rho_f}}{c_j} \right.$$
$$\left. - \frac{Z - Z_{j-1} + \frac{1}{2}H\frac{\rho}{\rho_f} + d_{j-1}\frac{\gamma_{j-1}}{\rho_f} + \frac{1}{2}H_{j-1}\frac{\rho_{j-1}}{\rho_f}}{c_{j-1}} \right\}, . \tag{4.21}$$

with A_n the surface of the vertex. The total correction flux can now be calculated by

$$Q_c^* = Q_v^* + Q_l^*. \tag{4.22}$$

4.3.4 FEM for the flow equation

The discretization of the correction flux q^* is explained in the previous section. The other terms of Equation (4.7) are also discretized with the finite element method. The matrices and vectors belonging to these terms can only be found in Triwaco's source code.

[30] [29]

Chapter 5

Numerical experiments

Consider the one dimensional problem with Dirichlet inflow boundary a and Neumann outflow boundary b:

$$\begin{cases} -\frac{\partial}{\partial x}\left(\theta D \frac{\partial C}{\partial x}\right) + q\frac{\partial C}{\partial x} + \theta\frac{\partial C}{\partial t} = q_{so}C_s; \\ C(a,t) = \alpha; \\ \theta D\frac{\partial C}{\partial x}(b,t) = \beta; \\ C(x,0) = C_0(x). \end{cases} \tag{5.1}$$

The region $[a,b] = [0,50]$ is subdivided into J equal parts with stepsize $\Delta x = 0.1$. The time interval $[0,T]$ is subdivided into N equal parts with timestep $\tau = 3$. As mentioned in Chapter 2, the dispersion coefficient $D = 0.003$, the advection coefficient $q = 0.03$. The porosity $\theta = 1$ and homogeneous boundary conditions are taken: $\alpha = \beta = 0$. Assume that there is no source, so $q_{so}C_s = 0$ and define the initial condition as

$$C_0(x) = \begin{cases} 0 & x \in [0,2]; \\ \frac{1-cos(\pi x)}{2} & x \in [2,4]; \\ 0 & x \in [4,6]; \\ 1 & x \in [6,8]; \\ 0 & x \in [8,50]. \end{cases} \tag{5.2}$$

Note that the CFL condition is satisfied: $|\frac{q\tau}{\Delta x}| \leq 1$.

5.1 Temporal discretization

Three different temporal discretizations are used: $T1$ is the temporal discretization that refers to the use of Backward Euler for the dispersion part and Forward Euler for the advection part and the source term (Equation (3.57)). $T2$ is the

temporal discretization that refers to the use of the Crank-Nicolson scheme (Equation (3.53)). $T3$ is the temporal discretization that refers to the use of the Runge-Kutta-2 scheme (Heun's method; Equation (3.59)).

Note that $T3$ does not have to be stable for the given parameters for the advection dispersion equation. $T3$ costs 2 calculation per time step, so in order to obtain the same computer work take a double step size for $T3$, $\Delta x = 0.2$ and take a look after 50 instead of 100 time steps. The results for the FEM, FVM and FDM can be found in the Figures 5.1, 5.2, 5.3. In Figure 5.4 the results can be found for the advection equation. It can be seen that $T1$ has less numerical dispersion than $T2$ and $T3$ which are the same for this example.

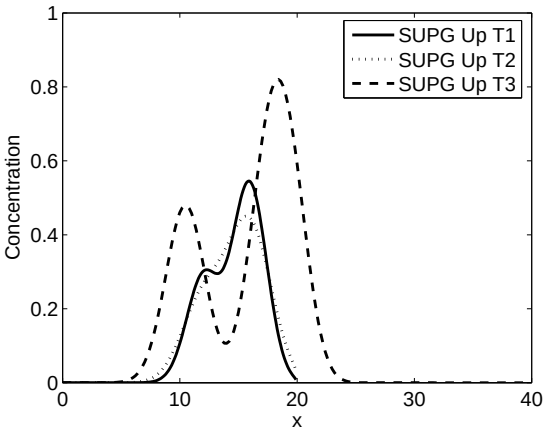

Figure 5.1: SUPG Up with $T1$ and $T2$ after 100 time steps with $\Delta x = 0.1$ and $T3$ after 50 timesteps with $\Delta x = 0.2$ for the advection dispersion equation.

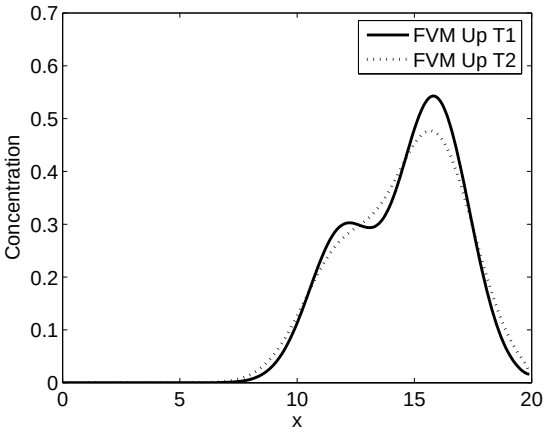

Figure 5.2: FVM Up with $T1$ and $T2$ after 100 time steps with $\Delta x = 0.1$ for the advection dispersion equation.

It can be seen that $T1$ has less numerical diffusion than method $T2$.

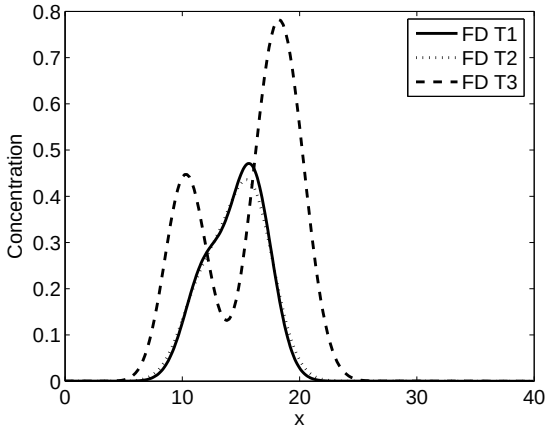

Figure 5.3: FDM with $T1$ and $T2$ after 100 time steps with $\Delta x = 0.1$ and $T3$ after 50 timesteps with $\Delta x = 0.2$ for the advection dispersion equation.

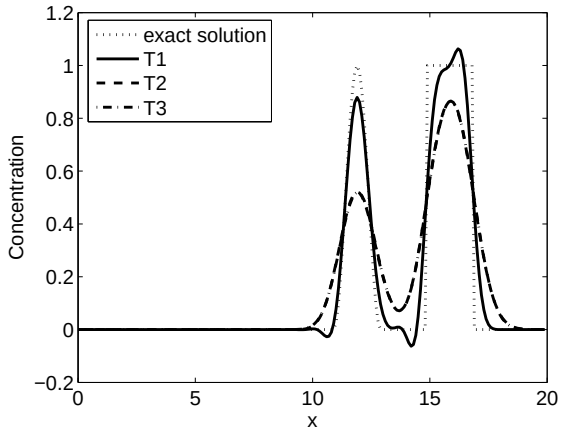

Figure 5.4: FEM CU with $T1$, $T2$ and $T3$ for the advection equation after 100 time steps.

?Remark?:$T3$ lijkt niet goed te werken, ik heb het volgende schema gebruikt:

$$\begin{aligned} \tfrac{M}{\tau} C_i^* &= \tfrac{M}{\tau} C_i^n + SC_i^n, \\ \tfrac{M}{\tau} C_i^{n+1} &= \tfrac{M}{\tau} C_i^n + \tfrac{1}{2} \left(SC_i^n + SC_i^* \right). \end{aligned} \tag{5.3}$$

kan dit slechts de onnauwkeurigheid zijn van een grotere plaatsstap?

5.2 Spatial discretization

For the Finite Element Method, the *Standard Galerkin Approach (SGA)* with the lumped mass matrix (*SGA* M_L) and the *Streamline Upwind Petrov-Galerkin (SUPG)* with different values for ξ:

$$\textit{Classical upwind scheme(SUPG CU):} \qquad \xi = sign(\alpha), \tag{5.4}$$

$$\textit{Il'in scheme (SUPG Il):} \qquad \xi = coth(\alpha) - 1/\alpha, \tag{5.5}$$

are presented as discussed in Section 3.2. The one dimensional derivation of the (element)matrices of these methods is given in Appendix E.

For the Finite Volume Method, the *first order upwind (FV Up)* method and the *MC limiter (MC)* are presented, see Section 3.3. For the Finite Difference Method (*FD*) only the first order upwind method is presented as discussed in Section 3.4. The matrices of these methods can be found in the Appendices F and G.

[6]

5.3 Advection Dispersion Equation

Results after 100 and 400 time steps with $T1$ for the finite element methods SGA M_L, SUPG CU and SUPG Il and the initial condition IC can be found in Figure 5.5.

Results after 100 and 400 time steps with $T1$ for the finite element method SGA with lumped mass matrix (SGA M_L) and consistent mass matrix (SGA M_C) can be found in in Figure 5.6.

Results after 100 and 400 time steps with $T1$ for the finite volume methods FV Up and MC and the finite difference method can be found in in Figure 5.7.

5.4 Advection Equation

5.4.1 Positive velocity

Choose $D = 0$ and $q = 0.03$ and note that the exact solution is $C(x,t) = f(x - qt)$, with $f(x)$ the initial condition. Results after 100 time steps can be found in Figures 5.9 and 5.10 for the FEM. The SGA is unstable and gives large wiggles. In Figure 5.11 the results for the FVM and FDM are shown.

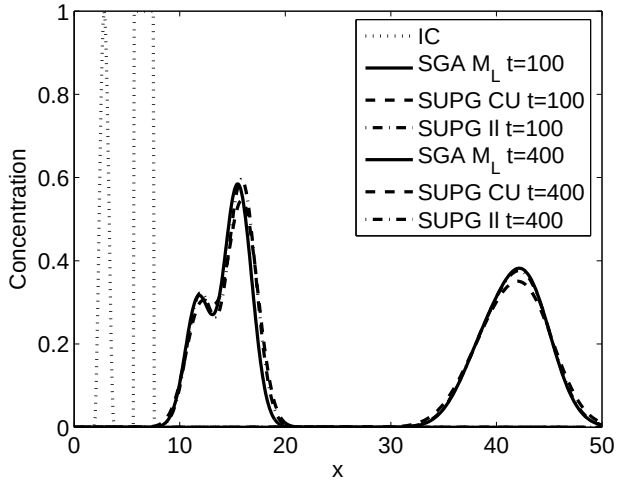

Figure 5.5: SGA M_L, SUPG CU and SUPG Il for the advection dispersion equation after 100 and 400 time steps with $T1$.

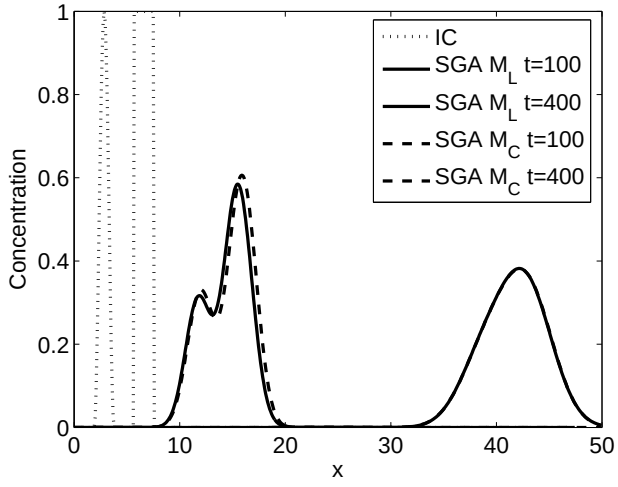

Figure 5.6: SGA M_L and SGA M_C for the advection dispersion equation after 100 and 400 time steps with $T1$.

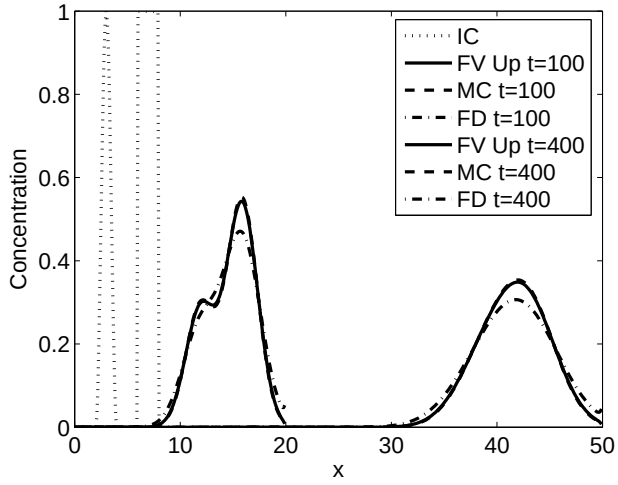

Figure 5.7: FV Up and FD with $T1$ and MC for the advection dispersion equation after 100 and 400 time steps.

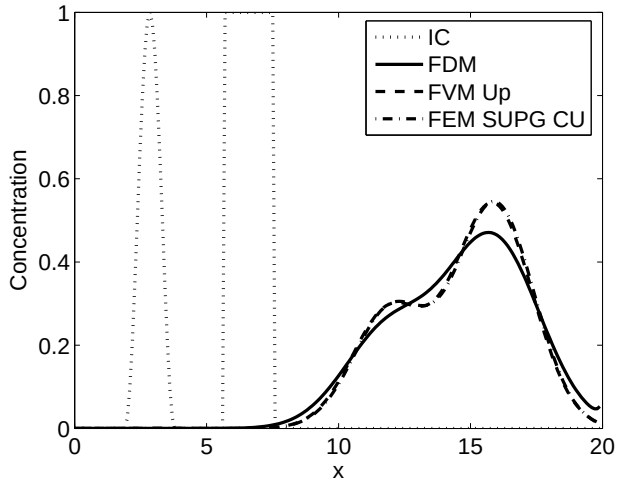

Figure 5.8: FEM, FDM and FVM for the advection dispersion equation after 100 time steps.

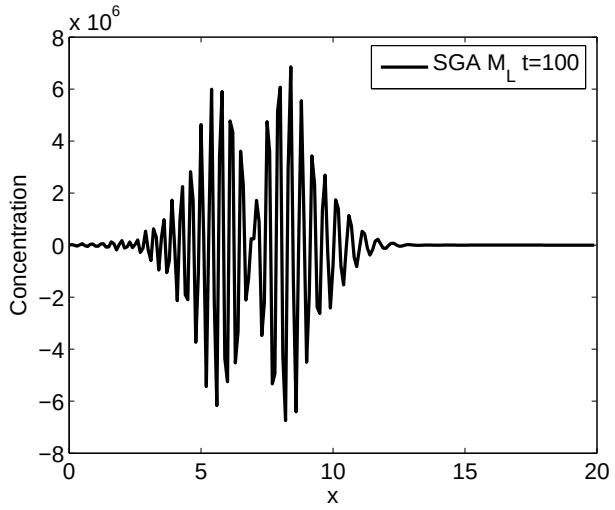

Figure 5.9: SGA M_L for the advection equation after 100 time steps with $T1$.

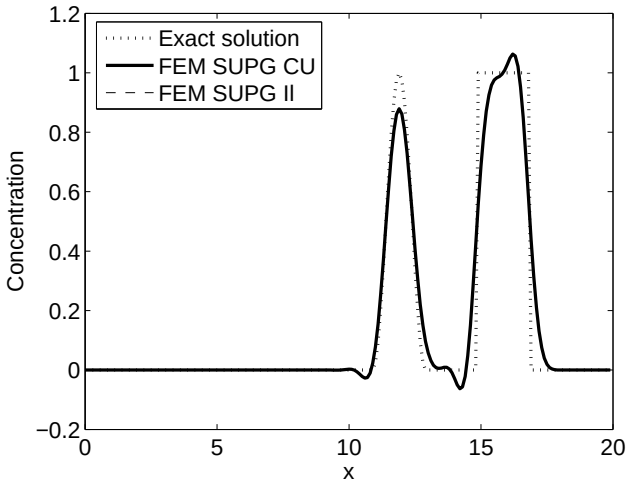

Figure 5.10: SGA SUPG CU and Il for the advection equation after 100 time steps with $T1$.

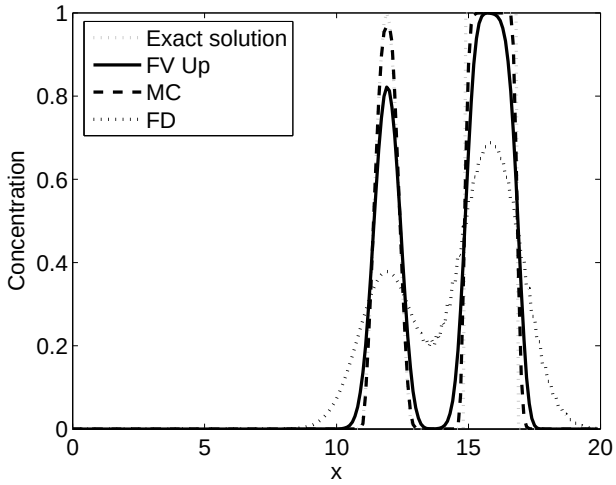

Figure 5.11: FVM and FDM for the advection equation after 100 time steps.

5.4.2 Negative velocity

Take the velocity $q = -0.03$, the dispersion coefficient $D = 0$ and the initial condition

$$C_0(x) = \begin{cases} 0 & x \in [0, 8]; \\ \frac{1-cos(\pi x)}{2} & x \in [8, 10]; \\ 0 & x \in [10, 12]; \\ 1 & x \in [12, 14]; \\ 0 & x \in [14, 50]. \end{cases} \tag{5.6}$$

All other parameters remain the same. In Figure 5.12 the results after 100 time steps with $T1$ can be found for the finite element method SUPG CU, the finite volume method FV Up and the finite difference method. The FEM SUPG Il gives the same result as FEM SUPG CU and the FEM SGA M_L and SGA M_C give results comparable with Figure 5.9.

5.5 Dispersion Equation

In Figure 5.13 the numerical results can be found for the advection equation. The numerical methods for the spatial discretization FEM, FVM and FDM and the methods for the temporal discretization $T1$, $T2$ and $T3$ act the same for this differential equation. As initial condition (5.2) is used.

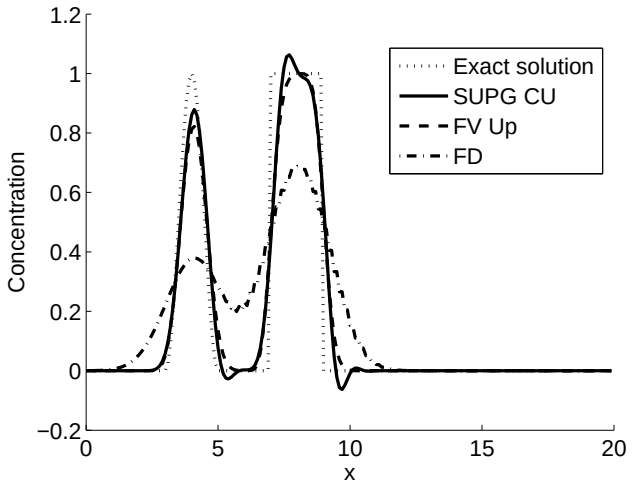

Figure 5.12: FEM SUPG CU and Il for the advection equation with negative velocity after 100 time steps.

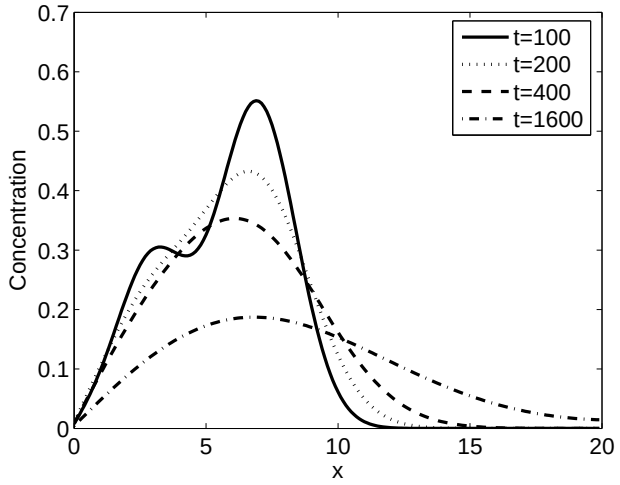

Figure 5.13: The numerical solution for the diffusion equation after 100, 200, 400 and 1600 time steps.

Chapter 6

Conclusions

6.1 Temporal discretization

	$T1$	$T2$	$T3$
stability condition	$\lvert\frac{q\tau}{\Delta x}\rvert \leq 1$	unconditionally stable	$\lvert\frac{q\tau}{\Delta x}\rvert \leq 1$ and $\frac{D\tau}{\Delta x^2} \leq \frac{1}{2}$
Accuracy	$O(\Delta t)$	$O(\Delta t^2)$	$O(\Delta t^2)$
Work	implicit scheme	implicit scheme	explicit but a two-step method
Numerical dispersion	Less	More	More

Table 6.1: Characteristics of the temporal discretization schemes Backward Euler for the dispersion part and Forward Euler for the advection part ($T1$), Crank-Nicholson ($T2$) and Runge-Kutta-2 ($T3$) for the 1D advection dispersion equation.

6.2 Spatial discretization

6.2.1 FEM

Advantages:

- The triangles of the finite element grid are more suitable for complex areas.

- In case of grid refinement the error stays small because in the FEM an integration is taken over the element (instead of the FVM where an evaluation of the concentration in one point is taken.)
- 'Parallel rekenen' is easier.
- The triangles (or in 3D prisms with triangular basis) are already used for the flow equation in Triwaco.

Disadvantages:

- There aren't simple higher order upwind methods.

6.2.2 FVM

Advantages:

- A higher order TVD method as the MC limiter is relatively easy to implement for 1D problems. For higher dimensions this advantage may disappear.

Disadvantages:

- Large error in case of grid refinement compared to FEM.

6.2.3 FDM

Advantages:

- Easy to implement.

Disadvantages:

- Numerical dispersion in the experimental problem.
- Large error in case of grid refinement compared to FEM.

6.2.4 IFALT

Advantages:

- No Peclet or Courant conditions.
- No time-stepping.
- Computationally efficient
- Low numerical dispersion

Disadvantages:

- Probably less accurate when applied to advective dominated flow.

	FEM			FVM		FD
	SGA	SUPG CU	SUPG Il	Up	MC	FD
Accuracy	$O(\Delta x)$	$O(\Delta x)$	$O(\Delta x)$	$O(\Delta x)$	$O(\Delta x^2)$	$O(\Delta x)$
Stable for the advection equation	No	Yes	Yes	Yes	Yes	Yes

Table 6.2: Characteristics of the different spatial discretization methods for the 1D advection dispersion equation.

Chapter 7

Future research

A method is needed that can solve the time dependent three dimensional advection dispersion equation, that suits easily in the used method for the flow equation in Triwaco, that is accurate and fast and can handle pure advection, pure dispersion, combinations and non-smooth initial conditions. The three stages of the future research will be:

- Link the advection dispersion equation with a simple method to the existing method for the flow equation in Triwaco, see Figure 2.4.
- Investigate higher order upwind finite element methods, for example comparable with the MC limiter for the FVM.
- Investigate analytical methods to solve the time-step, specially Laplace Transform (LT) for the time.

Bibliography

[1] *http://www.mnp.nl/en/publications/2006/TheeffectsofclimatechangeintheNetherlands.html.* website, August 2006.

[2] G.H.P. Oude Essink. *Impact of Sea Level Rise on Groundwater Flow Regimes.* Ph.D. thesis Delft University of Technology, Delft, 2006.

[3] W. Guo and C.D. Langevin. *User's guide to SEAWAT.* USGS, United States of America.

[4] C. van den Akker and H. Savenije. *Hydrologie 1 CT1310.* Delft University of Technology, Delft, 2006.

[5] M.P. Anderson and W.W. Woessner. *Applied Groundwater Modeling.* Academic Press, California, 1992.

[6] J. van Kan, A. Segal, and F. Vermolen. *Numerical Methods in Scientific Computing.* VSSD, Delft, 2004.

[7] J. Bear and Y. Bachmat. *Introduction to Modeling of Transport Phenomena in Porous Media.* Kluwer, Dordrecht, 1991.

[8] P.J. Stuyfzand. *Hydrochemistry and Hydrology of the Coastal Dune area of the Western Netherlands.* KIWA, Nieuwgein, 1993.

[9] A. Segal and C. Vuik. *Lecture notes Computational Fluid Dynamics 2, PhD course JM Burgerscentrum.* Delft University of Technology, Delft, 2004.

[10] C.W. Oosterlee and C. Vuik. *Scientific Computing.* Delft University of Technology, Delft, 2005.

[11] P. Clement and B. de Pagter. *Variationele methoden.* Delft University of Technoloty, Delft, 2003.

[12] D.C. Lay. *Linear algebra and its applications, second edition.* Addison-Wesley publishing company, USA, 2000.

[13] A.N. Brooks and T.J.R. Hughes. Streamline upwind/petrov-galerkin formulations for convection dominated flows with particular emphasis on the incompressible navier-stokes equations. *Computer methods in applied mechanics and engineering*, 32:199–259, 1982.

[14] R.J. Leveque. *Numerical Methods for Conservation Laws, Lectures Math. Birkhauser Verlag.* ETH Zurich, Zurich, 1992.

[15] R.J. Leveque. *Finite volume methods for hyperbolic problems.* Cambridge university press, Cambridge, 2002.

[16] A. Harten. High resolution schemes for hyperbolic conservative laws. *Journal of Computational Physics*, 49:357–385, 1983.

[17] D. Kuzmin and S. Turek. Finite element discretization and iterative solution techniquea for multiphase flows in gas-liquid reactors. *Proceedings of the Conference Finite Element Methods: 50 years of Conjugate Gradients*, 1, 2002.

[18] D. Kuzmin and S. Turek. *High-resolution FEM-TVD schemes based on a fully multidimensional flux limiter.* Institute of Applied Mathematics (LS III), University of Dortmund, Dortmund, 2003.

[19] P. Wesseling. *Principles of computational fluid dynamics.* Springer, New York, 1991.

[20] D. Kuzmin and D. Kourounis. *A semi-implicit FEM-FCT algorithm for efficient treatment of time-dependent problems.* Institute of Applied Mathematics (LS III), University of Dortmund, Dortmund, 2004.

[21] P. Wesseling. *Elements of computational fluid dynamics.* Delft University of Technology, Delft, 2002.

[22] T. Lowry and S.G. Li. A finite analytic method for solving the 2-d time-dependent advectiondiffusion equation with time-invariant coefficients. *Advances in Water Resources*, 28:117–133, 2005.

[23] T. Lowry and S.G. Li. A characteristic based finite analytic method for solving the two-dimensional steady-state advection-diffusion equation. *Water resources research*, 38:1–15, 2002.

[24] E. Sudicky. The laplace transform galerkin technique: a time-continuous finite element theory and application to mass transport in groundwater. *Water resources research*, 25:1833–1846, 1989.

[25] E. Sudicky. The laplace transform galerkin technique for efficient time-continuous solution of solute transport in double-porosity media. *Geoderma*, 46:209–232, 1990.

[26] E. Sudicky and R. McLaren. The laplace transform galerkin technique for large scale simulation of mass transport in discretely fractured porous formations. *Water resources research*, 28:499–514, 1992.

[27] J. Knight F. DeHoog and A. Stokes. An improved method for numerical inversion of laplace tansforms. *SIAM J Sci Stat Comput*, 3:357–366, 1982.

[28] T.N. Olsthoorn. Variable density groundwater flow modelling with modflow. *Proceedings Salt Water Intrusion Meeting SWIM 1996*, Malmo Sweden, 1996.

[29] W.J. Zaadnoordijk. *Variabele dichtheid in het eindige-elementengrondwaterstromingssimulatiepakket TRIWACO op basis van zoet-waterstijghoogten.* CiTG, Delft University of Technology, Delft, 1998.

[30] Royal Haskoning. *Triwaco User's manual*. Royal Haskoning, Nederland, 2004.

Appendix A

Used characters

Symbol	Definition	Dimension
q_i	flux in direction i	[m/d]
k	hydraulic conductivity	[m/s]
k_f	freshwater hydraulic conductivity	$[m/s]$
h	hydraulic head	[m]
h_f	freshwater head	[m]
ρ	density	$[kg/m^3]$
ρ_f	freshwater density	$[kg/m^3]$
κ	intrinsic permeability	$[m^2]$
S_s	specific storage	$[1/m]$
g	acceleration due to gravity	$[m/s^2]$
q'	volumetric flow rate per unit volume of aquifer representing sources and sinks	$[1/s]$
q_l	recharge due to leakage	$[1/s]$
q_r	recharge from rivers canals and drains	$[1/s]$
q_s	recharge from sources or sinks	$[1/s]$
q_a	recharge from the top-system (precipitations, shallow drainage system etc.)	$[1/s]$
μ	dynamic viscosity	$[kg/ms]$
μ_f	freshwater dynamic viscosity	$[kg/ms]$
Z	the height of the aquifer	$[m]$
C	concentration	$[kg/m^3]$
D	hydrodynamic dispersion coefficient	$[m^2/s]$
v	fluid velocity	$[m/s]$
q_{so}	volumetric flow rate per unit volume due to source/sink	$[1/s]$
C_s	solute concentration of water entering from sources or sinks	$[kg/m^3]$
θ	porosity	[-]
p	pressure	$[kg/ms^2]$

Appendix B

Definitions

Geohydrology

Anisotropic A porous medium is said to be anisotropic at a point with respect to a property if that property varies with direction at that point.

Aquifer Body of rock or sediment that is sufficiently porous and permeable to store, transmit and yield significant of economic quantities of groundwater to wells and springs. (watervoerende laag)

Aquitard A geologic formation that is not permeable enough to yield significant quantities of water to wells, but on a regional scale can contribute significant water to the underlying or overlaying aquifers. Only vertical velocity, the horizontal velocity of the flow is zero. (Waterscheidende laag)

Fresh water head The measured head if the piezometer tube were filled over its full height with water of specific weight.

Gauge pressure Pressure measured greater than atmospheric pressure

Hydraulic gradient Hydraulic head drop between two points a and b divided by the distance between them.

Hydraulic head Measure for the amount of energy groundwater flowing through aquifer has per unit weight. Quantity is expressed in terms of a length of water.

Hydrostatic pressure The pressure which is exerted on a portion of a column of fluid as a result of the weight of the fluid above it.

Phreatic The term phreatic is used in geology to refer to matters relating to underground water below the water table.

Phreatic zone The layer(s) of soil or rock below the water table in which voids are permanently saturated with water, as opposed to the higher vadose zone in which the pore spaces are not completely filled with water.

Piezometer A device used for the measurement of hydraulic head of groundwater in aquifers.

Pressure head Same as gauge pressure, unless absolute pressure is explicitly specified

Saturation Generally means water content is equal to porosity and pressure head is greater than atmospheric pressure. / The relative amount of water, oil and gas in the pores of a rock, usually as a percentage of volume

Specific Storage The amount of water which a given volume of aquifer will produce, provided a unit change in hydraulic head is applied to it (while it still remains fully saturated). it has units of inverse length, [L-1].

Transmissiviteit The rate at which water passes through an aquifer

Water table or phreatic surface The upper limit of abundant groundwater. The surface where the pressure head is equal to atmospheric pressure

Mathematics

Global truncation error The *global truncation error* is defined as

$$E^n \equiv C^n - C(n),$$

with C^n the numerical solution at $t = n$ and $C(n)$ the exact solution at $t = n$.

Local truncation error Scheme (3.53) can be written as $C^{n+1} = \mathcal{N}(C^n)$, where $\mathcal{N}$ represents the numerical operator mapping the approximate solution at one time step to the approximate solution at het next. The *local truncation error* is defined as

$$e^n = \frac{1}{\tau}[\mathcal{N}(C^n) - C^{n+1}].$$

Consistency Scheme (3.53) is called *consistent* if the local truncation error vanishes as $\tau \downarrow 0$ for all smooth functions $C(\mathbf{x}, t)$ satisfying the differential equation.

Stability A method is said to be *stable* if a small deviation from the true solution does not tend to grow as the solution is iterated.

Let $\{\delta_n, n = 0, 1, ..., N\}$ and $\{\delta_n^*, n = 0, 1, ..., N\}$ be any two perturbations of the discretized problem and let $\{\tilde{C}_n, n = 0, 1, ..., N\}$ and $\{\tilde{C}_n^*, n = 0, 1, ..., N\}$ be the resulting perturbed solutions. Then if there exist positive constant S and Δx_0 such that, for all $\Delta x \in (0, \Delta x_0]$:

$$||\tilde{C}_n - \tilde{C}_n^*|| \leq S\epsilon,$$

whenever

$$||\delta_n - \delta_n^*|| \leq \epsilon, \qquad 0 \leq n \leq N,$$

then the method is said to be zero-stable.

Convergence The method is *convergent* at time T in the norm $||.||$ if

$$lim_{\tau \to 0, N\tau = T} ||E^N|| = 0.$$

Here N is used to indicate the time level corresponding to time $T = N\tau$.

Laurent-series Zij G een gebied, f een functie die analytisch is op G, en $a \in C$, alsmede r en R zo gekozen dat $ann(a; r, R) = \{z \in \mathbb{C} : r < |z - a| < R\}$ niet leeg is en geheel in G ligt. Dan is f te ontwikkelen in een Laurentreeks:

$$f(z) = \sum_{n=-\infty}^{\infty} a_n (z-a)^n, \qquad z \in ann(a : r, R),$$

met *coëfficienten* a_n:

$$a_n = \frac{1}{2\pi i} \int_{\Gamma_\rho(a)} \frac{f(w)}{(w-a)n+1} dw$$

voor alle $n \in Z$, waarin ρ willekeurig is te kiezen zo dat $r < \rho < R$. De convergentie is absoluut voor alle z in de ring, en uniform op compacte deelverzamelingen van de ring. De voorstelling is bovendien uniek: Als $f(z)$ op de ring $ann(a; r, R)$ geschreven is als som van een Laurentreeks

$$f(z) = \sum_{n=-\infty}^{\infty} b_n (z-a)^n,$$

dan is dit vanzelf the Laurent series, d.w.z. $b_n = a_n$ voor alle n. [http://www.cs.vu.nl/ dijkstra/teaching/CF/CFdiktaat.pdf]

Appendix C

Experimental problems

Appendix D

software

Appendix E

1D Finite Element Methods

The discussed finite element methods are applied to the one dimensional problem and the matrices of the corresponding system of equations are given. Consider the one dimensional problem with inflow boundary a and outflow boundary b:

$$\begin{cases} -\frac{\partial}{\partial x}\left(\theta D \frac{\partial C}{\partial x}\right) + q\frac{\partial C}{\partial x} + \theta\frac{\partial C}{\partial t} = q_{so}C_s; \\ C(a,t) = \alpha; \\ \theta D\frac{\partial C}{\partial x}(b,t) = \beta; \\ C(x,0) = C_0(x). \end{cases} \tag{E.1}$$

The grid with a linear basis function can be found in Figure E. The lumped

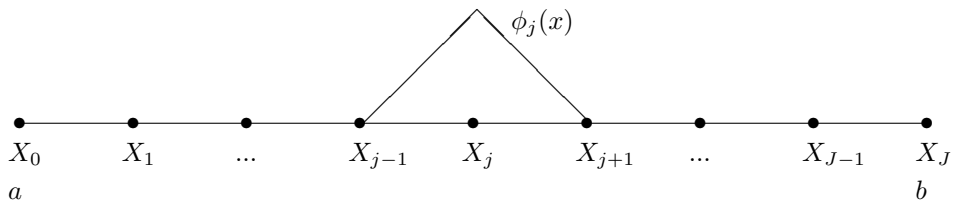

Figure E.1: The one dimensional Finite Element grid with a linear basis function.

mass-matrix M_L, the stiffness matrix S and the source vector f are derived with the Standard Galerkin Method as described in Chapter 3.2.3. Assume a constant step size Δx.

$$A = \begin{pmatrix} a_0^{k-1} & a_0^k \\ a_1^{k-1} & a_1^k \end{pmatrix}, X = \begin{pmatrix} 1 & x_1 \\ 1 & x_2 \end{pmatrix}, \tag{E.2}$$

$XA = I$, so

$$A = X^{-1} = \frac{1}{\Delta x}\begin{pmatrix} x_2 & -x_1 \\ -1 & 1 \end{pmatrix}. \tag{E.3}$$

Hence

$$\begin{aligned} \phi_{k-1}(x) &= a_0^{k-1} + a_1^{k-1}x = \tfrac{x_k - x}{\Delta x} \\ \phi_k(x) &= a_0^k + a_1^k x = \tfrac{-x_{k-1}+x}{\Delta x} \end{aligned} \tag{E.4}$$

and $d\phi_{k-1}/dx = -1/\Delta x$, $d\phi_k/dx = 1/\Delta x$. Note that in one dimension, the absolute value of the determinant of the matrix X is $|\Delta| = \Delta x$.

SGA
When the Newton-Cotes integration rule is used for the mass-matrix, a diagonal mass-matrix is obtained

$$M_L^{e_k} = \begin{pmatrix} m_{k-1,k-1}^{e_k} & m_{k-1,k}^{e_k} \\ m_{k,k-1}^{e_k} & m_{k,k}^{e_k} \end{pmatrix} = \begin{pmatrix} \frac{\Delta x}{2}\left(\theta(x_{k-1}) + \theta(x_k)\right) & 0 \\ 0 & \frac{\Delta x}{2}\left(\theta(x_{k-1}) + \theta(x_k)\right) \end{pmatrix}, \tag{E.5}$$

$$\begin{aligned} S^{e_k} &= \begin{pmatrix} s_{k-1,k-1}^{e_k} & s_{k-1,k}^{e_k} \\ s_{k,k-1}^{e_k} & s_{k,k}^{e_k} \end{pmatrix} = \\ &= \frac{-1}{2\Delta x}\begin{pmatrix} (\theta(x_{k-1})D(x_{k-1}) + & (-\theta(x_{k-1})D(x_{k-1}) - \\ +\theta(x_k)D(x_k) - \Delta x q(x_{k-1})) & \theta(x_k)D(x_k) + \Delta x q(x_{k-1})) \\ (-\theta(x_{k-1})D(x_{k-1}) - & (\theta(x_{k-1})D(x_{k-1}) + \\ \theta(x_k)D(x_k) - \Delta x q(x_k)) & +\theta(x_k)D(x_k) + \Delta x q(x_k)) \end{pmatrix}, \end{aligned} \tag{E.6}$$

$$f_i^{e_k} = \begin{pmatrix} f_{k-1}^{e_k} \\ f_k^{e_k} \end{pmatrix} = \begin{pmatrix} \frac{\Delta x}{2} q_{so}(x_{k-1})C_s(x_{k-1}) + \beta\phi_{k-1}(b) \\ -\frac{1}{2}\left(\theta(x_{k-1})D(x_{k-1})\alpha\frac{\partial\phi_0}{\partial x}|_{x_{k-1}} + \theta(x_k)D(x_k)\alpha\frac{\partial\phi_0}{\partial x}|_{x_{k-1}}\right. \\ \left. -q(x_{k-1})\alpha\frac{\partial\phi_0}{\partial x}|_{x_{k-1}}\right) \\ \\ \frac{\Delta x}{2} q_{so}(x_k)C_s(x_k) + \beta\phi_k(b) \\ -\frac{1}{2}\left(\theta(x_{k-1})D(x_{k-1})\alpha\frac{\partial\phi_0}{\partial x}|_{x_k} + \theta(x_k)D(x_k)\alpha\frac{\partial\phi_0}{\partial x}|_{x_k}\right. \\ \left. -q(x_k)\alpha\frac{\partial\phi_0}{\partial x}|_{x_k}\right) \end{pmatrix}. \tag{E.7}$$

Split the stiffness-matrix S^{e_k} into the matrix $S_1^{e_k}$ with the dispersive part and the matrix $S_2^{e_k}$ with the advective part, so $S = S_1 + S_2$. Substitution of the element matrices into the large $J \times J$ matrices M_L, S_1, S_2 and the $J \times 1$ vector f results in

$$M_L = \frac{|\Delta|}{2}\begin{pmatrix} \theta(x_1) + 2\theta(x_1) + \theta(x_2) & 0 & \cdots & 0 \\ 0 & \ddots & \ddots & \vdots \\ \vdots & \ddots & \theta(x_{J-2}) + 2\theta(x_{J-1}) + \theta(x_J) & 0 \\ 0 & \cdots & 0 & \theta(x_{J-1}) + \theta(x_J) \end{pmatrix}, \tag{E.8}$$

$$S_1 = -\frac{1}{2\Delta x}\begin{pmatrix} \theta(x_0)D(x_0) & -\theta(x_1)D(x_1) & & & \\ +2\theta(x_1)D(x_1) & -\theta(x_2)D(x_2) & 0 & . & 0 \\ +\theta(x_2)D(x_2) & & & & \\ -\theta(x_1)D(x_1) & \theta(x_1)D(x_2) & & & \\ -\theta(x_2)D(x_2) & +2\theta(x_2)D(x_2) & . & & 0 \\ & +\theta(x_3)D(x_3) & & & \\ 0 & \ddots & \ddots & \ddots & 0 \\ . & 0 & . & \theta(x_{J-1})D(x_{J-2}) & -\theta(x_{J-1})D(x_{J-1}) \\ & & & +2\theta(x_{J-1})D(x_{J-1}) & -\theta(x_J)D(x_J) \\ & & & +\theta(x_J)D(x_J) & \\ 0 & 0 & 0 & -\theta(x_{J-1})D(x_{J-1}) & \theta(x_{J-1})D(x_{J-1}) \\ & & & -\theta(x_J)D(x_J) & +\theta(x_J)D(x_J) \end{pmatrix}, \tag{E.9}$$

$$S_2 = \frac{1}{2}\begin{pmatrix} 0 & -q(x_1) & 0 & \cdots & 0 \\ q(x_2) & 0 & -q(x_2) & & \vdots \\ 0 & \ddots & \ddots & \ddots & 0 \\ \vdots & & q(x_{J-1}) & 0 & -q(x_{J-1}) \\ 0 & \cdots & 0 & q(x_J) & -q(x_J) \end{pmatrix}, \tag{E.10}$$

$$f = \begin{pmatrix} \frac{\Delta x}{2} q_{so}(x_1)C_s(x_1) + \frac{1}{2\Delta x}\left(\theta(x_0)D(x_0)\alpha + \theta(x_1)D(x_1)\alpha - \Delta x q(x_1)\alpha\right) \\ \Delta x q_{so}(x_2)C_s(x_2) \\ \vdots \\ \Delta x q_{so}(x_{J-1})C_s(x_{J-1}) \\ \frac{\Delta x}{2} q_{so}(x_J)C_s(x_J) + \beta \end{pmatrix}. \tag{E.11}$$

In order to obtain a non-lumped or consistent mass-matrix the integrals are calculated directly. The element matrix becomes:

$$M_C^{e_k} = \begin{pmatrix} \int_{\Delta x}\theta(x_{k-1})\phi_{k-1}\phi_{k-1}d\Omega & \int_{\Delta x}\theta(x_k)\phi_k\phi_{k-1}d\Omega \\ \int_{\Delta x}\theta(x_{k-1})\phi_{k-1}\phi_k d\Omega & \int_{\Delta x}\theta(x_k)\phi_k\phi_k d\Omega \end{pmatrix} \tag{E.12}$$

$$\cong \begin{pmatrix} \theta(x_{k-1})\Delta x/2 & \theta(x_k)\Delta x/2 \\ \theta(x_{k-1})\Delta x/2 & \theta(x_k)\Delta x/2 \end{pmatrix}, \tag{E.13}$$

so the large consistent mass-matrix is

$$M_C = \Delta x \begin{pmatrix} 2\theta(x_1) & \theta(x_2) & 0 & \cdots & 0 \\ \theta(x_1) & 2\theta(x_2) & \theta(x_3) & & \vdots \\ 0 & \ddots & \ddots & \ddots & 0 \\ \vdots & & \theta(x_{J-2}) & 2\theta(x_{J-1}) & \theta(x_J) \\ 0 & \cdots & 0 & \theta(x_{J-1}) & \theta(x_J) \end{pmatrix}. \tag{E.14}$$

SUPG
The SUPG method in one dimension is the normal upwind method. The equation to be solved is

$$\int_\Omega \left(\frac{\partial w}{\partial x}(\theta D \frac{\partial C}{\partial x}) + (q\frac{\partial C}{\partial x})w + \theta \frac{\partial C}{\partial t} w \right) d\Omega + \sum_{k=1}^{n_e} \int_{\Omega^{e_k}} \left\{ q\frac{\partial C}{\partial x} + \theta \frac{\partial C}{\partial t} \right\} b d\Omega =$$
$$= \int_\Omega q_{so} C_s w d\Omega + \int_{\Gamma_2} g_2 w d\Gamma + \sum_{k=1}^{n_e} \int_{\Omega^{e_k}} q_{so} C_s b d\Omega, \tag{E.15}$$

with

$$b = \frac{\Delta x}{2} \xi \frac{d\phi_i}{dx}. \tag{E.16}$$

ξ determines the choice of the SUPG method, as discussed in Section 3.2.3. The elements described in the Equations (3.11), (3.12) and (3.13) become

$$m_{ij} = \sum_{k=1}^{n_e} \int_{\Omega^{e_k}} \theta(x_j)\phi_j \left(\phi_i + \frac{\Delta x}{2} \xi \frac{d\phi_i}{dx} \right) d\Omega, \tag{E.17}$$

$$s_{ij} = -\sum_{k=1}^{n_e} \int_{\Omega^{e_k}} \left(\frac{\partial \phi_i}{\partial x} \left(\theta(x_j) D(x_j) \frac{\partial \phi_j}{\partial x} \right) + \left(\mathbf{q}(x_j) \frac{\partial \phi_j}{\partial x} \right) \left(\phi_i + \frac{\Delta x}{2} \xi \frac{d\phi_i}{dx} \right) \right) d\Omega, \tag{E.18}$$

$$f_= \sum_{k=1}^{n_e} \int_{\Omega^{e_k}} (q_{so} C_s)(\mathbf{x}_j) \left(\phi_i + \frac{\Delta x}{2} \xi \frac{d\phi_i}{dx} \right) d\Omega + \sum_{k=1}^{n_{be_2}} \int_{\Gamma_2^{e_k}} g_2(\mathbf{x}_j)\phi_i d\Gamma$$
$$- \sum_{k=1}^{n_e} \int_{\Omega^{e_k}} \sum_{j=n+1}^{n+n_B} (\nabla \phi_i \cdot (\theta D g_1(\mathbf{x}_j) \nabla \phi_j)$$
$$+ (\mathbf{q} \cdot (\alpha) \frac{d\phi_0}{dx})) \left(\phi_i + \frac{\Delta x}{2} \xi \frac{d\phi_i}{dx} \right) d\Omega. \tag{E.19}$$

The matrix M now exists of the sum of two matrices, the lumped mass-matix M_L or the consistent matrix M_C and the mass-matrix M_U of the upwind part:

$$M_U^{e_k} = \begin{pmatrix} \int_{\Delta x} \theta(x_{k-1})\phi_{k-1} \frac{\Delta x}{2} \xi \frac{d\phi_{k-1}}{dx} d\Omega & \int_{\Delta x} \theta(x_k)\phi_k \frac{\Delta x}{2} \xi \frac{d\phi_{k-1}}{dx} d\Omega \\ \int_{\Delta x} \theta(x_{k-1})\phi_{k-1} \frac{\Delta x}{2} \xi \frac{d\phi_k}{dx} d\Omega & \int_{\Delta x} \theta(x_k)\phi_k \frac{\Delta x}{2} \xi \frac{d\phi_k}{dx} d\Omega \end{pmatrix} \tag{E.20}$$

$$= \begin{pmatrix} -\theta(x_{k-1}) \frac{\Delta x}{4} \xi & -\theta(x_k) \frac{\Delta x}{4} \xi \\ \theta(x_{k-1}) \frac{\Delta x}{4} \xi & \theta(x_k) \frac{\Delta x}{4} \xi \end{pmatrix}, \tag{E.21}$$

Note that the consistent upwind mass-matrix equals the upwind mass matrix derived with the Newton-Cotes rule. The stiffness-matrix S now consists of the sum of S and the extra upwind part S_U:

$$S_U^{e_k} = \begin{pmatrix} q(x_{k-1})\frac{\xi}{2} & -q(x_{k-1})\frac{\xi}{2} \\ \\ q(x_k)\frac{\xi}{2} & -q(x_k)\frac{\xi}{2} \end{pmatrix}. \tag{E.22}$$

The vector f exists of the sum of the vector (E.7) and the upwind part f_U:

$$f_U^{e_k} = \begin{pmatrix} -\frac{\Delta x}{2}\xi\left(q_{so}(x_{k-1})C_s(x_{k-1}) + q(x_{k-1})\alpha\frac{d\phi_0}{dx}\right) \\ \\ \frac{\Delta x}{2}\xi\left(q_{so}(x_k)C_s(x_k) + q(x_k)\alpha\frac{d\phi_0}{dx}\right) \end{pmatrix}. \tag{E.23}$$

Appendix F

Matrices Finite Volume Methods

option 1 The use of central differences for the dispersive flux (Equation (3.68)), first order upwind for the advective flux (Equation (3.69)) and the temporal discretization scheme of Equation (3.67) results in a system of equation of the form $AC^{n+1} = BC^n + f$ with

NOTE: graphicx package geinstalleerd om rotatebox/sideways te kunnen gebruiken, maar dit werkt niet

$$A = \begin{bmatrix} 1+\frac{\tau}{\Delta x_1\theta_1}\left(\frac{\theta_{3/2}D_{3/2}}{\Delta x_{3/2}}+\frac{\theta_{1/2}D_{1/2}}{\Delta x_{1/2}}\right) & -\frac{\tau}{\Delta x_1\theta_1}\frac{\theta_{3/2}D_{3/2}}{\Delta x_{3/2}} & 0 & \cdots & 0 \\ -\frac{\tau}{\Delta x_2\theta_2}\frac{\theta_{3/2}D_{3/2}}{\Delta x_{3/2}} & 1+\frac{\tau}{\Delta x_2\theta_2}\left(\frac{\theta_{5/2}D_{5/2}}{\Delta x_{5/2}}+\frac{\theta_{3/2}D_{3/2}}{\Delta x_{3/2}}\right) & \ddots & & \vdots \\ 0 & \ddots & \ddots & \ddots & 0 \\ \vdots & & \ddots & \ddots & -\frac{\tau}{\Delta x_J\theta x_J}\frac{\theta_{J+1/2}D_{J+1/2}}{\Delta x_{J+1/2}} \\ 0 & \cdots & 0 & -\frac{\tau}{\Delta x_J\theta_J}\frac{\theta_{J+1/2}D_{J+1/2}}{\Delta x_{J+1/2}} & 1+\frac{\tau}{\Delta x_J\theta_J}\left(\frac{\theta_{J+1/2}D_{J+1/2}}{\Delta x_{J+1/2}}+\frac{\theta_{J-1/2}D_{J-1/2}}{\Delta x_{J-1/2}}\right) \\ & & & & -\frac{\tau\theta_{J+1/2}D_{J+1/2}}{(\Delta X_J)^2\theta_J} \end{bmatrix}, \tag{F.1}$$

$$B = \begin{bmatrix} 1-\frac{\tau}{\Delta x_1\theta_1}\left(\frac{1}{2}\left(q_{3/2}+|q_{3/2}|\right)+\left(q_{1/2}-|q_{1/2}|\right)\right) & -\frac{\tau}{\Delta x_1\theta_1}\frac{1}{2}(q_{3/2}-|q_{3/2}|) & 0 & \cdots & 0 \\ \frac{\tau}{\Delta x_2\theta_2}\frac{1}{2}(q_{3/2}+|q_{3/2}|) & 1-\frac{\tau}{\Delta x_2\theta_2}\left(\frac{1}{2}\left(q_{5/2}+|q_{5/2}|\right)+\left(q_{3/2}-|q_{3/2}|\right)\right) & \ddots & & \vdots \\ 0 & \ddots & \ddots & \ddots & 0 \\ \vdots & & \ddots & \ddots & -\frac{\tau}{\Delta x_J\theta_J}\frac{1}{2}(q_{J+1/2}-|q_{J+1/2}|) \\ 0 & \cdots & 0 & \frac{\tau}{\Delta x_J\theta_J}\frac{1}{2}(q_{J+1/2}+|q_{J+1/2}|) & 1-\frac{\tau}{\Delta x_J\theta_J}\left(\frac{1}{2}\left(q_{J+1/2}+|q_{J+1/2}|\right)+\left(q_{J-1/2}-|q_{J-1/2}|\right)\right)-\frac{\tau}{\Delta x_J\theta_J}(1/2(q_{J+1/2}-|q_{J+1/2}|) \end{bmatrix} \tag{F.2}$$

$$f^n = \begin{bmatrix} \left(\frac{q_{so}C_s}{\theta}\right)_1^n - \frac{\tau}{\Delta x_1\theta_1}\frac{\theta_{1/2}D_{1/2}}{\Delta x_1}\alpha - \frac{\alpha\tau}{2\Delta x_1\theta_1}(q_{1/2}+|q_{1/2}|) \\ \left(\frac{q_{so}C_s}{\theta}\right)_2^n \\ \vdots \\ \left(\frac{q_{so}C_s}{\theta}\right)_{J-1}^n \\ \left(\frac{q_{so}C_s}{\theta}\right)_J^n + \frac{\tau\beta\theta_{J+1/2}D_J}{\theta_J} + \frac{\tau\beta\ D_J}{\theta_J}(1/2(q_{J+1/2}-|q_{J+1/2}|)) \end{bmatrix}, \tag{F.3}$$

Appendix G

Finite Difference matrices

$$M = \begin{bmatrix} \theta_1 & 0 & \cdots & 0 \\ 0 & \theta 2 & \ddots & \vdots \\ \vdots & \ddots & \ddots & \vdots \\ 0 & \cdots & 0 & \theta_J \end{bmatrix}, \tag{G.1}$$

with $\theta_i = \frac{\theta_{i+1/2}+\theta_{i-1/2}}{2}$

$$S_1 = \frac{1}{\Delta x^2} \begin{bmatrix} -2\theta_1 D_1 & \tilde{\tilde{\theta D}}_1 & 0 & \cdots & 0 \\ \tilde{\theta D}_2 & -2\theta_2 D_2 & \tilde{\tilde{\theta D}}_2 & \ddots & \vdots \\ 0 & \ddots & \ddots & \ddots & 0 \\ \vdots & \ddots & \ddots & \ddots & \tilde{\tilde{\theta D}}_{J-1} \\ 0 & \cdots & 0 & \tilde{\theta D}_J + \tilde{\tilde{\theta D}}_J & -2\theta_J D_J \end{bmatrix}, \tag{G.2}$$

with

$$\tilde{\theta D}_i = \frac{\theta_i D_i}{(\Delta x)^2} - \frac{1}{2(\Delta x)^2}\left(\theta_i(D_{i+1/2} - D_{i-1/2}) + D_i(\theta_{i+1/2} - \theta_{i-1/2})\right)$$

and

$$\tilde{\tilde{\theta D}}_i = \frac{\theta_i D_i}{(\Delta x)^2} + \frac{1}{2(\Delta x)^2}\left(\theta_i(D_{i+1/2} - D_{i-1/2}) + D_i(\theta_{i+1/2} - \theta_{i-1/2})\right)$$

and $D_i = \frac{D_{i+1/2}+D_{i-1/2}}{2}$

$$S_2 = \begin{bmatrix} -\frac{sign(q_1)q_1}{2\Delta x} & 0 & -\frac{q_1-|q_1|}{4\Delta x} & 0 & \cdots & 0 \\ 0 & -\frac{sign(q_2)q_2}{2\Delta x} & 0 & -\frac{q_2-|q_2|}{4\Delta x} & \ddots & \vdots \\ \frac{q_3+|q_3|}{4\Delta x} & 0 & -\frac{sign(q_3)q_3}{2\Delta x} & \ddots & \ddots & 0 \\ 0 & \ddots & \ddots & \ddots & 0 & -\frac{q_{J-2}-|q_{J-2}|}{4\Delta x} \\ \vdots & \ddots & \ddots & \ddots & \ddots & \frac{q_{J-1}-|q_{J-1}|}{4\Delta x} \\ 0 & \cdots & 0 & \frac{q_J+|q_J|-(q_J-|q_J|)}{4\Delta x} & 0 & -\frac{sign(q_J)q_J}{2\Delta x} \end{bmatrix}, \tag{G.3}$$

with $q_i = \frac{q_{i+1/2}+q_{i-1/2}}{2}$,